# Dynamic Flow Priming Programs Allow Tuning Up The Cell Layers Properties for Engineered Vascular Graft.

**Kazutomo Baba** ( baba@golem.iit.tsukuba.ac.jp )
University of Tsukuba
**Andrey Mikhailov**
University of Tsukuba
**Yoshiyuki Sankai**
University of Tsukuba

**Research Article**

**Keywords:** Tissue engineered vascular graft (TEVG), bioreactor system, fibroblast layer, biocompatible glass

**Posted Date:** December 28th, 2020

**DOI:** https://doi.org/10.21203/rs.3.rs-134799/v1



**Version of Record:** A version of this preprint was published at Scientific Reports on July 19th, 2021. See the published version at https://doi.org/10.1038/s41598-021-94023-9.

# Dynamic flow priming programs allow tuning up the cell layers properties for engineered vascular graft.

Kazutomo Baba [1*], Andrey Mikhailov [2] and Yoshiyuki Sankai [2, 3]

[1]Graduate School of Systems and Information Engineering, University of Tsukuba, 1-1-1 Tennodai, Tsukuba-shi, Ibaraki 305-8573, Japan, [2]Center for Cybernics Research, University of Tsukuba, Japan, [3]Faculty of Engineering, Information and Systems, University of Tsukuba, Japan
*Corresponding author: baba@golem.iit.tsukuba.ac.jp

## Abstract

Tissue engineered vascular graft (TEVG) has a good potential to replace and repair demanded blood vessels. Here, we proposed a novel method to create three-layered TEVG on biocompatible glass fiber scaffolds starting from flat sheet state into tubular shape and to train the resulting tissue by our developed bioreactor system. Constructed tubular tissues were matured and trained under 3 types of individual flow programs, and their mechanical and biological properties were analyzed. The strength of scaffold after cell seeding was 2.83 N which is sufficient to withstand the pressure of blood flow and the use of sutures. Fluorescent imaging and histological examination of trained vascular tissue revealed that each cell layer has its own individual response to training flow rates. Fluid flow simulation model was created based on experimentally measured tissue geometries; its analysis suggested a correlation between local flow rate fluctuations and fibroblast layer infiltration depth into the scaffold. Concluding: a three-layered tissue structure similar to natural can be created by seeding different cell types in succession, and the following training of the forming tissue with increasing flow by a bioreactor is effective for promoting cell survival, and cell layer formation of desired geometry.

## Introduction

Until recently, small artificial vascular prostheses, less than 6mm in diameter, could not be used clinically due to lack of their antithrombotic and infection resistance and high chance of early occlusion[1–4]. When arteriosclerotic vascular disorders including ischemic heart disease, peripheral artery disease, or similar conditions occur, in some cases catheter treatment or stenting may not be possible, then surgical revascularization such as coronary artery bypass grafting or lower limb bypass surgery is required. Regular treatment of choice is utilizing the patient's own blood vessels, such as the internal thoracic artery or the great saphenous vein[5]. However, often in the patients with arterial disease, other blood vessels in their body are affected by stenosis as well, which makes it difficult to harvest a healthy vein necessary for bypass surgery[6].

Vascular graft therapy based on tissue engineering is a treatment option in such cases[7]. Since tissue engineered vascular graft (TEVG) have good potential to replace and repair demanded areas, several approaches to construct TEVG were suggested so far[8]. Self-organization methods such as cell-sheet, micro tissue aggregation, or 3D bio-printing are scaffold-free methods utilizing only the cells[9–11]. They have common advantage of biocompatibility, yet each method has its own limitations. Cell sheets method allow to mimic the layered structure of blood vessels by stacking one sheet at a time. However, the stacking of dense sheets of cells disrupt the supply of nutrients and oxygen to the interior layer[12]. Micro tissue aggregation is reliable method for tissue formation in required size and we previously developed a method and the bioreactor for its implementation to form tubular tissue of arbitrary diameter and length[13]. However, it is challenging to control the self-assembly of the cells, and no one has not yet been able to reproduce a natural vessel with a correct three-layered structure by this approach. 3D bio-printing could make layer structure in principle, however, since gravity applied in the height direction, the stacked length is actually limited whether a bio-printer handles individual cells or spheroids as a single

dispensing unit[14]. Another challenge of 3D cell printing is cell viability due to extrusion pressure[15].

The clinical application of TEVG requires reconstruction of vascular function based on the three-layered tissue structure, as well as scalability in size and the strength to withstand blood flow pulses and surgery suturing, but it is still difficult and timely to satisfy all these requirements with just self-assembly approaches in current technologies. In this study, rather than relying only on self-assembly, we proposed a method to form natural vascular layer structure with biocompatible glass fibers and developed a novel bioreactor and housing devices which allow to form the cell layers, to mature the layer structure, and to train the assembled vascular tissues with various perfusion flow. In addition, we examined mechanical and biological features of the constructed tubular tissue and the relationship between the properties of the composed layers and the training flow rate inside the bioreactor.

## Results

### Layer structure formation during sheet culture period

Cells were seeded onto sterilized glass fiber sheets placed into silicon frames of our design (Fig.1) allowing media access from both sides of the sheets. Layers of cells on glass fiber sheets were assembled in following succession: fibroblasts (NHDFc), red fluorescent protein (RFP) expressing Human Aortic Smooth Muscle Cells (hASMCs), and green fluorescent protein (GFP) expressing Human Umbilical Vein Endothelial Cells (HUVECs). Fibroblast showed invasive growth with penetration of the material (Fig.2A); hASMCs and HUVEC formed cell layers on top of previously seeded cells (Fig.2B, 2C).

### Cell density and viability

Count of DAPI stained nuclei (Fig.3A) of cells in NHDFc layer was compared quantitatively with results of staining with Calcein AM and Ethidium (Fig.3B). Cell borders in 3D tissue image were overlapping, so staining with Calcein AM cannot be used for calculation of the cell number, only for visualization of live cells prevalence. Table.1 shows the number of cells averaged over 5 images, their density, and cell viability calculated from these results. Most of the cells' nuclei were negative for ethidium and the survival rate was estimated at 95.8 $\pm$ 1.4 %.

### The changes of the mechanical strength of glass fiber during tissue formation

There was little change in the strength of the glass fiber itself before and after autoclaving with subsequent 2 weeks long immersion in the culture media (Fig.4). On the other hand, glass fiber sheets after seeding and growing the fibroblasts lost the strength significantly ($p<0.001$). The strength of the glass fiber sheets decreased from 11.56 $\pm$ 1.98 N in the dry state to 2.83 $\pm$ 0.76 N in fibroblast-infiltrated samples. We expect that invasive growth of the fibroblasts into the depth of glass fiber (Fig.5) disturbed connections between the fibers and so its strength.

### Tubular structure formation and tissue removal

Glass fiber sheets with 3 cell layers were successfully rounded into a tube shape by the proposed method with help of sterilized metal rod 3.5mm in diameter and the shape was stabilized with surgical suture. Tubular proto-tissues were placed into 4-channels bioreactor of our design and matured by individual training flow programs. Complete cycle of training and maturation took two weeks. Although, some experimental procedures such as removal of the formed tissue from the system, cutting it with scissors, washing the tissue with PBS, and pinching with tweezers were challenging to perform, we visually confirmed in most of the cases that the tubular shape could be retained without much damage (Fig.6). After crosscut, the tissues were placed into transparent plastic dishes, and live fluorescence observation of the vascular tissue was performed in the cross-sectional direction. We can observe that the shape of tissue was close to tubular, and green fluorescent endothelial cells could be seen inside the red fluorescent smooth muscle cells layer (Fig.7A). Stronger layer of endothelial cells could be seen in samples with different training program as on Fig.7B, where endothelial cells spread more evenly on the hASMCs

layer and the two layers had defined separation.

### Histological analysis

21 cross-cut synthetic vascular tissues were stained with HE to confirm histologically the fusion and organization of each cell layer and to calculate each layer's thickness (Fig.8). The effects of the perfusion flow rate on the maturation of tissue layer structure were analyzed. We compared stationary cultured rounded sheets with the same sheets trained under final flow rates 1,2 and 5 ml/min. As shown in Fig.9, each layer has its own individual response to flow rate alterations. The thickness of all cell layers increased when the flow was applied compared to the stationary culture. The same situation occurs in all types of cells comprising our tissues, suggesting that sustained nutrient and oxygen delivery by the bioreactor and associated mechanical training allowed the cells to increase their number and area. On the other hand, as the flow rate increases, the thickness of cell layers reached apex at a certain point individual on each cell type and began to decrease especially for the endothelial cells and the fibroblasts at higher rates.

### Flow simulation

To address the reasons for observed strength reduction in relation to the effects of cellular infiltration, and profile of the material and flow velocity distribution of our bioreactor, a 3D model was created from series of the actual tissue shapes obtained during experiments. Crosscut profiles were copied from the actual HE-stained cross sections (for example Fig.5), and subsequently a fluid simulation was performed (Fig.10). The media velocity was higher in the center of the vessel and it decrease as approaches the wall forming a gradient. The relationship between the simulated fluid velocity at 15 points on the inner surface of the tissue and the thickness of the cell layer at those points is shown in Fig.11. The curves represent the results of the logarithmic approximation. The Spearman's rank correlation coefficient between tissue thickness of fibroblast layer and flow velocity is 0.76 suggesting a strong dependence.

## Discussion

Small diameter conventional artificial vascular grafts have major limitations with respect to thrombosis, infection, and biocompatibility. Extensive research is being conducted to develop small-diameter TEVGs using regenerative medicine and tissue engineering approaches[8,16,17]. The supply of nutrients and oxygen has always been recognized as an important issue in the development of three-dimensional tissues[18]. Moreover, since natural blood vessels are constantly exposed to blood flow, it is particularly important to consider the effect of mechanical stimulation during *in vitro* culture[19]. Bioreactor-based culture systems hold the potential to provide a testing platform that is more predictable of a whole tissue response by providing more physiologically relevant conditions comparing to customarily used two- and three-dimensional cultures[20,21]. Here we proposed a novel method to create three-layered TEVG with biocompatible glass fibers as supporting scaffold and to train a tissue by the developed bioreactor system. Constructed tubular tissues were matured and trained under 3 types of individual flow, and we compared their mechanical and biological features.

In current study, we utilized glass fiber sheet as the scaffold. The grass fiber has good biocompatibility and previous studies have shown that it can be applied safely in animals[22,23]. Our selected grass fiber sheets satisfied all of the following specifications required for constructing three layered blood vessel; (1) biocompatibility - to avoid foreign body reactions and rejection, (2) negligible cytotoxicity – to ensure proper cell survival, (3) surface allowing cell adhesion - to facilitate mechanical support, (4) porosity for nutrients and oxygen supply, (5) flexibility permitting sheet-to-tube folding, and (6) sufficient material strength to withstand the experimental manipulation and blood pressure fluctuations. The glass fiber sheets we used consist of a porous material with a particle retention capacity of 2.7 μm, which allow seeding cell layers with suspension of the individual cells. Material has sufficient permeability for the culture medium, and it has the flexibility to be formed into a tube shape (Fig.6).

Similar attempt combining cell sheet engineering and electrospinning technology was performed, and bioreactor preconditioned SMC sheet-combined vascular scaffold maintained high cell viability (95.9 ± 2.7%), phenotypes and improved cellular infiltration, as well as desired mechanical properties[9]. We confirmed that the cells were uniformly attached and spread along the fibrous direction (Fig.2). The survival rate of the cells was pretty good (95.8%). From these results, we suggested that porous grass fiber sheet is useful as a biocompatible material for tissue preparation. Certainly, it lacks biodegradability, so future developments should be aimed for use of biodegradable glasses[23–25] which were not available for us in a form of fiber filters at the time of our study.

Besides glasses, other materials were used for cellular support in TEVG. Crosslinked electrospun gelatin scaffolds of specific fibre layer orientation was developed, and high suture retention strength was achieved in the range of 1.8–1.94 N for wet acellular scaffolds, same or better than that for fresh saphenous vein[26]. The tensile strength measurements of our scaffold showed that there was little change in strength between dry and soaked material, however strength was dramatically reduced after cell culture. Nevertheless, vascular tissue with grass fiber scaffold has a tensile strength of 2.83 N, which is sufficient to withstand the pressure of blood flow and the use of sutures.

Formation of the three-layered structure on the glass fiber seeded with differentiated primary cells of three types was confirmed, and the assembled layer order was maintained during all incubation period in the tube shape. As an alternative to primary cells, differentiated iPS cells can provide an attractive cell source for constructing TEVGs using the sheet engineering technique[27]. Recent article reported generation of hiPSC-derived TEVGs with mechanical strength comparable to native vessels used in arterial bypass grafts by utilizing biodegradable scaffolds, incremental pulsatile stretching, and optimized culture conditions[28]. On the other hand, the technology to assemble sheets of endothelial cells and fibroblasts derived from iPS cells with SMCs has not yet been realized, it seems to be still difficult to form a multilayered vascular structure using a pipe-like scaffold (including molds). The sheet-to-tube folding using glass fiber scaffold with multiple cell types gave the advantage of creating a three-layered structure in intended order and maintaining it after formation of the tube.

Regarding cell organization in the scaffold, each layer thickness tended to decrease as the flow rate reached maximum. There are several possibilities to explain the phenomenon: For example, if the flow is too fast some cells at the inner surface (endothelial) could be mechanically flushed away. We were able to recover some green fluorescent cells from circulation, but it was difficult to perform quantitative measurements. The same tendency was observed for red fluorescent smooth muscle cells, but not as drastic as for endothelial cells. In a literature, a pulsatile flow bioreactor was developed to allow shear and pulsatile stimulation of TEVGs constructed from with 10T-1/2 mouse smooth muscle progenitor cells[29]. Authors discovered that the constructs subjected to 7 weeks of biomechanical conditioning had significantly higher collagen levels and improved moduli relative to those grown under static conditions. In our case, the smooth muscle cells were sandwiched between endothelial cells and fibroblasts, which made them less affected by shear stress.

The thickness of fibroblast layer has decreased significantly as well as endothelial cells. When the glass fiber was rolled, the inner surface was sometimes slightly wrinkled, which caused dimples to appear outward from the circular tube (as shown as a white dotted line in the center in Fig.10). The reduction in flow speed, mainly around the wrinkles shown by our simulation, would result in a more depleted oxygen supply to the cells. The histological analysis (Fig.5) revealed that the cells infiltrating the glass fibers were almost exclusively fibroblasts. Systematic computer simulations and parametric studies of different types of scaffolds in the dynamic bioreactor showed predicted oxygen concentration profiles at the center of the pore in a fibrous scaffold, and predicted cell front propagation distance from the seeded surface of the scaffold[30]. Simulations showed that cells fill the pores of the porous scaffold over a period of days, and the oxygen concentration decreases on a log-like scale as the distance from the seeded surface increases[30]. In our case, there is a near-log-scale increase in cell invasion when the flow velocity is reduced (i.e. the oxygen supply is reduced). Overall thickness variation was higher at lower flow rate. These evidences suggest that the flow velocity optimal for fibroblasts to create a structure close to naturally occurring is different from the other two cell types. Although our result indicated high cell viability, this could be due to supplying the culture medium from both outside and inside the scaffold. The outer microflow is thought

to be similar to the capillary function that enters the outer walls of arteries in the body. Calculations predict that in case of circulation limited to inside area, the maximum cell propagation would be about half of the current level (0.4 to 0.45 mm), and we can expect limited viability of cell in areas that have infiltrated deeply into the scaffold.

Our comparison of modelled flow and histological structure of the tissue points to invasion of fibroblast cell into glass fiber scaffold in area of slower flow and, perhaps, lower mass rate exchange between circulated media and forming tissue. Is it an influence of lower oxygen tension, nutrients concentration or waste products insufficient removal? Interplay between cell oxygen tension and physiological responses (migration in particular) is not known in details and some data are controversial. For example, cultured L929 fibroblasts under hypoxic conditions (1% $O_2$) demonstrated enhanced cell spreading, decrease of single cell migration, and a decline of cell motility[31]. 24 hr hypoxia exposure govern fibrotic responses in cardiac fibroblasts: their proliferation, secretion of inflammatory and pro-fibrotic cytokines in culture supernatants; myofibroblast differentiation[32]. Indirectly attributed to migration is finding that low oxygen tension coupled with macromolecular crowding significantly accelerate extracellular matrix deposition and the development of scaffold-free tissue-like modules. Interestingly, fibroblasts exhibited the highest metabolic activity at slightly hypoxic conditions - 2% oxygen tension and more extracellular matrix proteins - collagens type I, V, and VI and fibronectin were deposited at 2% oxygen tension, as opposed to 0.5% and 20%[33].

On the other hand, some of the observed effects might be attributed to effective exchange between media and trained tissue in area with higher flow velocity. It was demonstrated that high glucose conditions (25 mM D-glucose, or about 4500 mg/L in fresh media we used) inhibited cell migration when compared to low glucose concentration[34]. Comparing behavior of several types of the cells at different oxygen and glucose concentrations authors have found that survival of fibroblasts was higher at slightly hypoxic conditions (5%) comparing to both severe hypoxia (0.1%) or normoxia (21% of oxygen in gas mix)[35].

From these results, some insights and limitations for future development can be suggested. A three-layered tissue structure can be created by seeding the cells in sequence using a sheet-like porous glass fiber scaffold. Then rounding is possible, and training of forming tissue with increasing flow by a bioreactor is effective for promoting cell survival and proliferation. At that time, selecting individually and providing the proper flow rate is important factor for the cell layer formation close to naturally occurring. Excessive flow lead to detachment and washing away of cells: insufficient lead to improper layer structure. Different flow delivery to both the inner and outer sides could be one potential option for cell type-specific layer construction and organization.

## Methods

### Cells

We used 3 types of cells normally comprising blood vessels: Fibroblasts (NHDFc, C-12302, PromoCell, Heidelberg, Germany), Smooth muscle cells (hASMCs, cAP-0026RFP, Angio-Proteomie, Boston, USA), and Endothelial cells (HUVECs, cAP-0001GFP, Angio-Proteomie, Boston, USA). Frozen stock of each types of the cells was melted and scaled up in appropriate media: D-MEM (High Glucose with Phenol Red and Sodium Pyruvate, StemSure®, Wako) supplemented with 10% of fetal calf serum for smooth muscle cells and fibroblasts and Endothelial media (Endothelial Cell Growth Medium, PromoCell) for endothelial cells in 75cm$^2$ flasks (Primaria, Corning, NC, USA). Before co-culture cells were adapted for 1:1 mix of the above media for 72hr. For layer formation cells were detached from the surface with Trypsin/EDTA solution (Wako, Japan), and washed with its cultured media filtered through 1.2 um membrane filter.

### Scaffold

We used glass fiber filters (Whatman grade GF/D / GE Healthcare) for cell support and formation of the tubular shapes after. Filters were cut into pieces (16.5 x 20 mm), sterilized by autoclaving and soaked with cell culture media 24-hour prior the cell seeding.

### The Silicon frame design for cell seeding on glass fiber scaffold

The cells in suspension have similar density to their culture media, so forming the cell layer on flat sheet in bigger Petri dish led to escape of sizeable part of seeded cells from intended surface. Therefore, a PDMS silicon frame was developed to accommodate the glass fiber sheet (Fig.1). The size of the glass fiber sheet was set 16.5 x 20 mm which can form a tubular shape with 4 mm inner diameter, 6 mm outer diameter, and 20 mm length when it is bent into the tube. When the mold was submerged inside the dish, the culture medium could permeate from both top and bottom.

### Biocompatibility

Since we used glass fiber supporting scaffold, which was not specifically designed for cell attachment, ensuring its biocompatibility was necessary prior to further experiments. Evaluation of the biocompatibility was done by seeding NHDFc on sterilized filters and measuring cell viability after 7 days growth with LIVE/DEAD® Viability/Cytotoxicity Kit (Molecular Probes / Thermo-Fischer). Since projections of cell bodies on 3D scaffold are heavily overlapped, we used DAPI staining to count the total cell number and staining with Ethidium homodimer to assess the number of dead cells with damaged membrane (necrotic and late apoptotic cells). For each measurement we used 5 separate field of view, calculation was done with ImageJ software[36].

### Tensile strength measurements

We developed a holder for comparative measurement of dry and wet glass fiber sheets before and after tissue formation (Fig.12A). Tensile strength of glass fiber was measured using the holder of our own design, Load/Displacement Measurement Unit (FSA-1KE-20N, IMADA, Japan), and digital force gauge (ZTA-20N, IMADA, Japan) shown in Fig.12B, in order to verify whether the strength of glass fiber was changed by infiltration of the culture medium. The filter (n=4) was wrapped around the axel in terminal holders and increasing pulling force applied according to the internal program. We measured 3 sets of filters: factory dry, sterilized and kept wet, and filters with cells.

### The three-layered structure formation of tissue engineered blood vessels

To mimic natural structure of blood vessel we propose a method in which the culture process is divided into stages as illustrated in Fig.13. First, the fibroblast (NHDFc) layer, which is the outer layer of vessels, was seeded on top of the pretreated glass fiber. We used about $10^7$ cells. One week after the media was changed and the next layer was formed with hASMCs, and after another week the same operation repeated with HUVECs. For maturation of three-layered tissue, we used additional 7 days with two media changes during that period.

### Bioreactor and training system

Our bioreactor system consists of a control unit, an autoclavable perfusion pump unit (WPM2-P3EA-CP / Welco), a gas exchange unit, 4-channels vascular training unit, and shared media reservoir (Fig.14). Every component except the control unit were sterilized by autoclaving. The size of entire system is 30 cm length, 20 cm width, and 17 cm height, and whole device was installed inside a CO2 incubator during entire culture period.

The control unit consists of a main circuit board which regulate the flow rate and reads sensor values, stepper motors, motor drivers (L6470 / STMicroelectronics), temperature and humidity sensor, polycarbonate housing, and a rubber sealing frame. This unit adjust a flow rate of the perfusion pump unit between 0~48 ml/min. Four stepper motors have daisy-chained each other and allow to support individual flow control or batch synchronous control. Since each circulation pathway of the media is mechanically independent, it allows to perform and analyze the cultivations under individual flow conditions. The flow rate and its procedure of changing up to the target value can be set by the user via an external serial communication port.

The gas exchange unit consists of four silicon tubes (3mm inner diameter) of about 2 m long wrapped around the supporting stand and it is connected between the shared reservoir and each training unit. The media

passing through this unit delivers oxygen to cells due to reasonable gas permeability of silicon as well as stabilize carbon dioxide level necessary for maintenance of pH buffer capacity of the culture media.

4-channels vascular training unit consist of silicon tube housings (8 mm diameter), several luer connectors, and the supporting stand. The culture medium transported from the pump passes mainly through the inner side of the tubular tissue installed in the silicone housing. Media flows allow to mature proto-tissues and to give the shear stress for the training of cell-to-cell adhesion and extra cellular matrix adaptation. A slight gap between the outside of the tubular tissue and the housing provided flow of the culture medium, supplying oxygen and nutrients to the cells through the glass fiber scaffold material.

### Tubular shape formation by developed auxiliary device

After confirming by life fluorescent microscopy of the flipped over filter that the smooth muscle cells and the endothelial cells layers have been formed, we returned filters in upright position and placed them in fresh media. Forming of continuously round shape for glass fiber filter with attached cell layers is challenging. Therefore, we developed an auxiliary device for ensuring safety and reproducibility of the glass fiber wrapping (Fig.15). In this device, a sheet is placed on the stage first, then a metal pipe (3.5mm diameter) is placed on the sheet and fixed to both tube ends, and the tubular shape could be initialized and maintained by wrapping the glass fiber sheet with two silicon belts. At this state, the glass fiber sheet around the tube is tied and fixed at three of more points with surgical sutures. With this assistive device, the operation could be completed in 5-10 minutes per one tissue to avoid the tissue drying.

The tissues then were placed into sterilized silicone tube housing and connected into the bioreactor system we have developed. Culture medium circulated through the housing for two weeks with changing of 50% of the media to the fresh one every 120hr. As a result, tissues were subjected to shear stress and tension from the fluid in the similar way as blood vessels in the body, which was expected to promote cell-to-cell adhesion and a reinforcing mechanical stress response.

### Maturation and training of the tissue in the developed bioreactor

Four equal glass fiber sheets with 3 cell layers were prepared for each experiment. They were placed inside the silicon tube housings in the system, sealed with connectors, and the individual flow supplied from the individually programmed pumps to reach 1.0, 2.0, and 5.0 ml during 72 hours, and then the maturation and training was continued at the steady flow rate for 2 more weeks (Fig.16).

### Live imaging

The distribution of cells in the inner part of the trained tubular tissues was assessed by help of fluorescent proteins expressed in smooth muscle cells (red) and endothelial cells (green). Tubular tissues with surrounding glass fiber scaffold were crosscut, washed with warm PBS and placed in Petri dishes under the layer of PBS on inverted fluorescence microscope (Nikon eclipses Ti). Several images were acquired with different depth of focus and restored by Adobe Photoshop into single combined image.

### Histological evaluation

The tissues removed from bioreactor housing were washed with warm PBS, and fixed in 4% paraformaldehyde in phosphate buffer for 20 min at 37 ℃. The fixed tissues were sent to external processing (New Histo Science Laboratory Co. Ltd., Tokyo, Japan) for sectioning and staining. HE stained slides were photographed and thickness of different cell layers estimated in quadruplicates for each image.

### Flow simulation

A 3D model of the blood vessel was created using CAD (SOLIDWORKS® 2018 / Dassault Systèmes SolidWorks Corporation), and the shapes were digitized from our actual HE stained histological sections. Fluid analysis of that model was also performed using SOLIDWORKS® Flow Simulation incorporated in the same software. The

calculation area was defined as the silicon tubes of the training unit and internal whole tissues. Boundary conditions were set at 2 ml/min flow rate at the inlet and 101325 Pa and 293.2 K of static pressure at the outlet.

## References


1. Isenberg, B. C., Williams, C. & Tranquillo, R. T. Small-diameter artificial arteries engineered in vitro. *Circ. Res.* **98**(1), 25–35 (2006).
2. Teebken, O. E. & Haverich, A. Tissue engineering of small diameter vascular grafts. *Eur. J. Vasc. Endovasc. Surg.* **23**(6), 475–485 (2002).
3. Zilla, P., Bezuidenhout, D. & Human, P. Prosthetic vascular grafts: Wrong models, wrong questions and no healing. *Biomaterials* **28**(34), 5009–5027 (2007).
4. Baquey, C. Developments towards tissue- arterial substitutes. *Tissue Eng.* **5**(3), 337–347 (2008).
5. Faries, P. L. *et al.* A comparative study of alternative conduits for lower extremity revascularization: All-autogenous conduit versus prosthetic grafts. *J. Vasc. Surg.* **32**(6), 1080–1090 (2000).
6. Gerhard-Herman, M. D. *et al.* 2016 AHA/ACC guideline on the management of patients with lower extremity peripheral artery disease: Executive Summary: A report of the American college of cardiology/American Heart Association task force on clinical practice guidelines. *Circulation* **135**(12), e686–e725 (2017).
7. Pashneh-Tala, S., MacNeil, S. & Claeyssens, F. The tissue-engineered vascular graft - Past, present, and future. *Tissue Eng. - Part B Rev.* **22**(1), 68–100 (2016).
8. Carrabba, M. & Madeddu, P. Current strategies for the manufacture of small size tissue engineering vascular grafts. *Front. Bioeng. Biotechnol.* **6** 41 (2018).
9. Ahn, H. *et al.* Engineered small diameter vascular grafts by combining cell sheet engineering and electrospinning technology. *Acta Biomater.* **16**(1), 14–22 (2015).
10. Kelm, J. M. *et al.* A novel concept for scaffold-free vessel tissue engineering: Self-assembly of microtissue building blocks. *J. Biotechnol.* **148**(1), 46–55 (2010).
11. Itoh, M. *et al.* Scaffold-free tubular tissues created by a bio-3D printer undergo remodeling and endothelialization when implanted in rat aortae. *PLoS One* **10**(9), 1–15 (2015).
12. Rademakers, T., Horvath, J. M., van Blitterswijk, C. A. & LaPointe, V. L. S. Oxygen and nutrient delivery in tissue engineering: Approaches to graft vascularization. *J. Tissue Eng. Regen. Med.* **13**(10), 1815–1829 (2019).
13. Baba, K., Mikhailov, A. & Sankai, Y. Combined automated culture system for tubular structure assembly and maturation for vascular tissue engineering. *J. Biomech. Sci. Eng.* **13**(3), 1–14 (2018).
14. Duan, B. State-of-the-Art Review of 3D Bioprinting for Cardiovascular Tissue Engineering. *Ann. Biomed. Eng.* **45**(1), 195–209 (2017).
15. Thattaruparambil Raveendran, N., Vaquette, C., Meinert, C., Samuel Ipe, D. & Ivanovski, S. Optimization of 3D bioprinting of periodontal ligament cells. *Dent. Mater.* **35**(12), 1683–1694 (2019).
16. Ratcliffe, A. Tissue engineering of vascular grafts. *Matrix Biol.* **19**(4), 353–357 (2000).
17. Radke, D. *et al.* Tissue Engineering at the Blood-Contacting Surface: A Review of Challenges and Strategies in Vascular Graft Development. *Adv. Healthc. Mater.* **7**(15), 1–24 (2018).
18. McMurtrey, R. J. Analytic models of oxygen and nutrient diffusion, metabolism dynamics, and architecture optimization in three-dimensional tissue constructs with applications and insights in cerebral organoids. *Tissue Eng. - Part C Methods* **22**(3), 221–249 (2016).
19. Song, H. H. G., Rumma, R. T., Ozaki, C. K., Edelman, E. R. & Chen, C. S. Vascular Tissue Engineering: Progress, Challenges, and Clinical Promise. *Cell Stem Cell* **22**(3), 340–354 (2018).
20. Massai, D. *et al.* Bioreactor Platform for Biomimetic Culture and in situ Monitoring of the Mechanical Response of in vitro Engineered Models of Cardiac Tissue. *Front. Bioeng. Biotechnol.* **8** 733 (2020).
21. Peroglio, M., Gaspar, D., Zeugolis, D. I. & Alini, M. Relevance of bioreactors and whole tissue cultures for the translation of new therapies to humans. *J. Orthop. Res.* **36**(1), 10–21 (2018).
22. Jeans, L. A., Gilchrist, T. & Healy, D. Peripheral nerve repair by means of a flexible biodegradable glass fibre wrap: A comparison with microsurgical epineurial repair. *J. Plast. Reconstr. Aesthetic Surg.* **60**(12), 1302–1308 (2007).
23. Starritt, N. E., Kettle, S. A. J. & Glasby, M. A. Sutureless repair of the facial nerve using biodegradable glass fabric. *Laryngoscope* **121**(8), 1614–1619 (2011).
24. Burova, I. *et al.* A parameterised mathematical model to elucidate osteoblast cell growth in a phosphate-glass microcarrier culture. *J. Tissue Eng.* **10** https://doi.org/10.1177/2041731419830264 (2019).
25. Colquhoun, R. & Tanner, K. E. Mechanical behaviour of degradable phosphate glass fibres and composites - A

review. *Biomed. Mater.* **11**(1), (2015).
26. Elsayed, Y., Lekakou, C., Labeed, F. & Tomlins, P. Fabrication and characterisation of biomimetic, electrospun gelatin fibre scaffolds for tunica media-equivalent, tissue engineered vascular grafts. *Mater. Sci. Eng. C* **61** 473–483 (2016).
27. Hibino, N. *et al.* Evaluation of the use of an induced puripotent stem cell sheet for the construction of tissue-engineered vascular grafts. *J. Thorac. Cardiovasc. Surg.* **143**(3), 696–703 (2012).
28. Luo, J. *et al.* Tissue-Engineered Vascular Grafts with Advanced Mechanical Strength from Human iPSCs. *Cell Stem Cell* **26**(2), 251-261.e8 (2020).
29. Hahn, M. S., McHale, M. K., Wang, E., Schmedlen, R. H. & West, J. L. Physiologic pulsatile flow bioreactor conditioning of poly(ethylene glycol)-based tissue engineered vascular grafts. *Ann. Biomed. Eng.* **35**(2), 190–200 (2007).
30. Elsayed, Y., Lekakou, C. & Tomlins, P. Modeling, simulations, and optimization of smooth muscle cell tissue engineering for the production of vascular grafts. *Biotechnol. Bioeng.* **116**(6), 1509–1522 (2019).
31. Vogler, M. *et al.* Hypoxia Modulates Fibroblastic Architecture, Adhesion and Migration: A Role for HIF-1 $\alpha$ in Cofilin Regulation and Cytoplasmic Actin Distribution. *PLoS One* **8**(7), e69128 (2013).
32. Ugolini, G. S. *et al.* Human cardiac fibroblasts adaptive responses to controlled combined mechanical strain and oxygen changes in vitro. *Elife* **6** 1–20 (2017).
33. Kumar, P., Satyam, A., Cigognini, D., Pandit, A. & Zeugolis, D. I. Low oxygen tension and macromolecular crowding accelerate extracellular matrix deposition in human corneal fibroblast culture. *J. Tissue Eng. Regen. Med.* **12**(1), 6–18 (2018).
34. Lamers, M. L., Almeida, M. E. S., Vicente-Manzanares, M., Horwitz, A. F. & Santos, M. F. High glucose-mediated oxidative stress impairs cell migration. *PLoS One* **6**(8), 1–9 (2011).
35. Lafosse, A., Dufeys, C., Beauloye, C., Horman, S. & Dufrane, D. Impact of hyperglycemia and low oxygen tension on adipose-derived stem cells compared with dermal fibroblasts and keratinocytes: Importance for wound healing in type 2 diabetes. *PLoS One* **11**(12), 1–18 (2016).
36. Schneider, C. A., Rasband, W. S. & Eliceiri, K. W. NIH Image to ImageJ: 25 years of image analysis. *Nat. Methods* **9**(7), 671–675 (2012).

## Acknowledgments

This research was funded by ImPACT Program, promoted by Council for Science, Technology and Innovation, Cabinet Office, Japan.

## Author Contributions

K. B. equipment design and pilot production, experiment, analysis, writing, editing. A. M. experiment, analysis, writing, editing. Y. S. project administration, supervision, review, editing.

## Competing interests

The authors declare no competing interests.

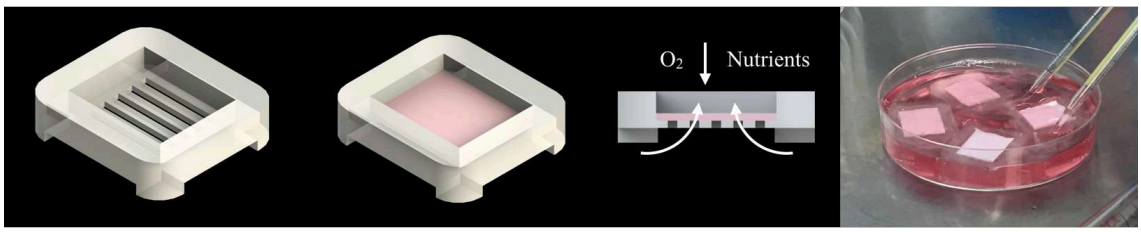


**Figure 1.** Silicone frame design for a glass fiber sheet set up and cell layer formation. Far right: Actual frames with glass fiber scaffold preconditioned in culture media.

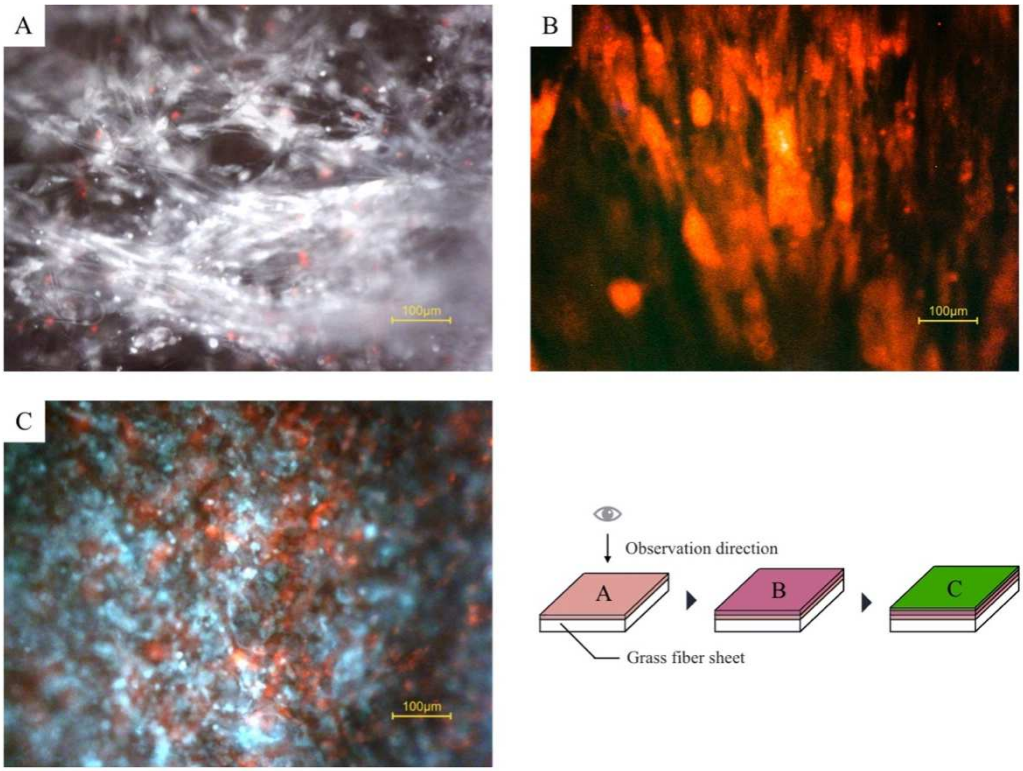


**Figure 2.** Formation of the tissue layers on a glass fiber sheet at each maturation step during sheet culture period. (A) First layer, white: fibroblasts stained by Calcein-AM, red: dead cells stained by ethidium, (B) Second layers, red fluorescent: RFP-SMCs. Fibroblasts on the background are non-fluorescent, (C) Third layers, red: RFP-SMCs, teal: GFP-HUVECs with automatic white balance. Each picture was taken under inverted fluorescent microscope after completing tissue maturation steps at weekly intervals. Fig.2C endothelial cell layer (blue) is in front of the smooth muscle cell layer (red), and the cells are close to uniformly distributed on the glass fiber.

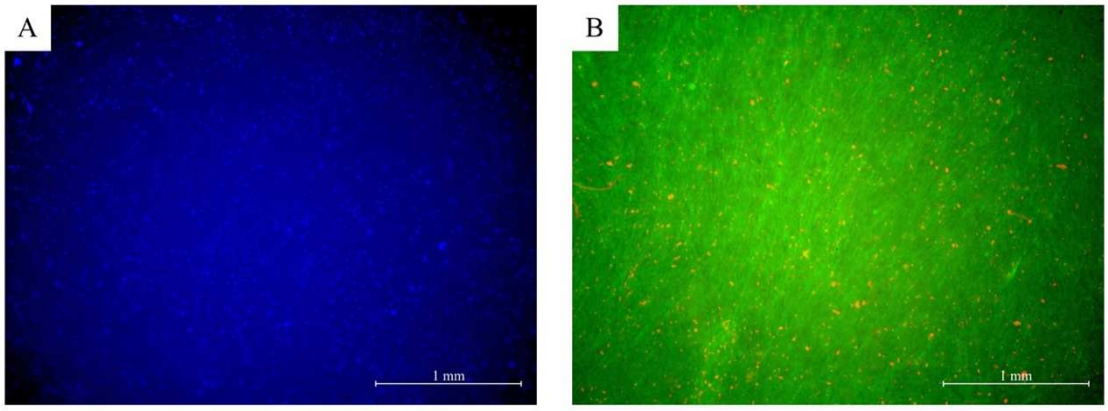


**Figure 3.** Survival of cells in the formed tissues on a GF sheet after maturation by the developed bioreactor. (A) DAPI stained nuclei, (B) Staining with Calcein-AM and Ethidium.

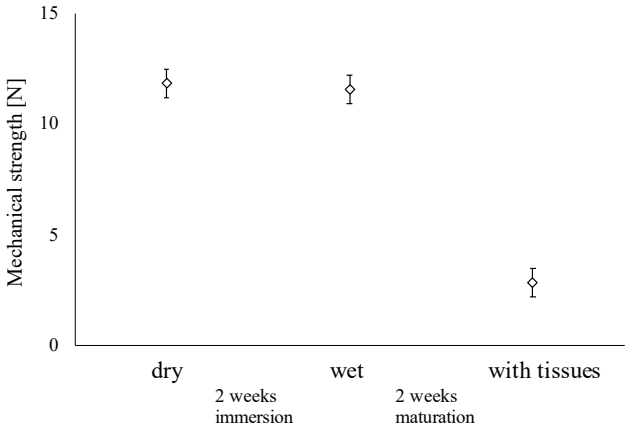


**Figure 4.** Strength measurement of the grass fiber sheet before and after tissue formation with the developed tensile tester device.

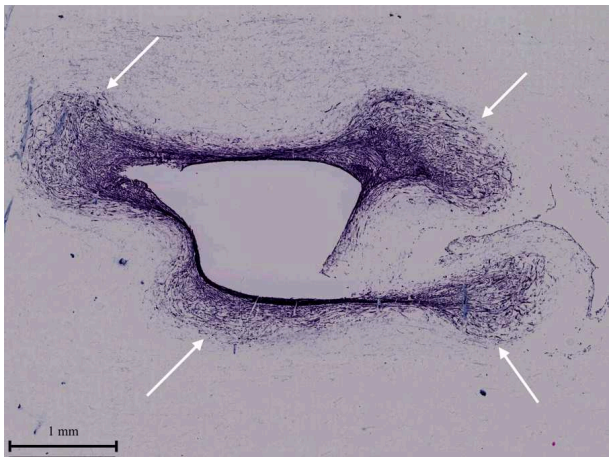


**Figure 5.** Infiltration of fibroblasts into a glass fiber. white allows: invasive growth areas.

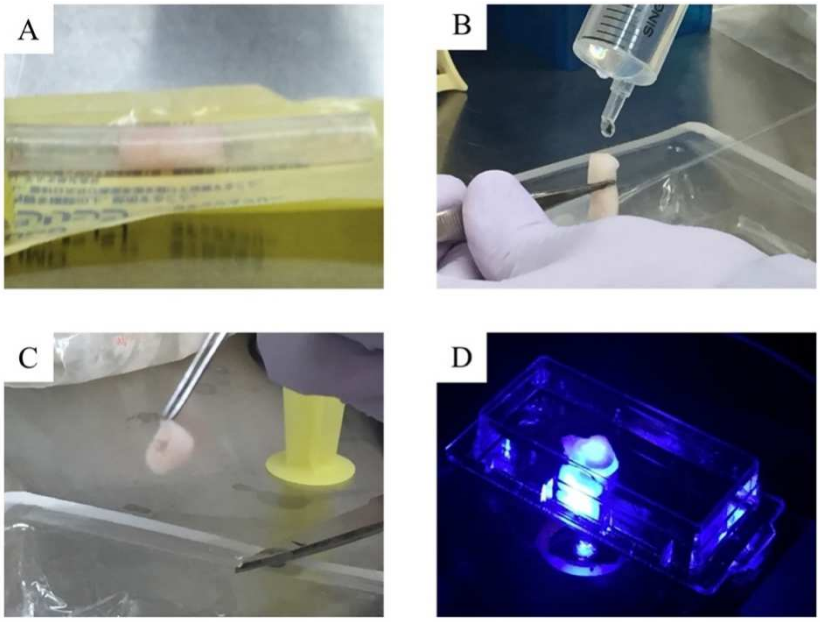


**Figure 6.** Matured blood vessels after training in the bioreactor. The tubular shape could be retained without much damage by some experimental procedures. (A)Extraction (B) Washing with PBS (C) Cutting/Slicing (D) Observation

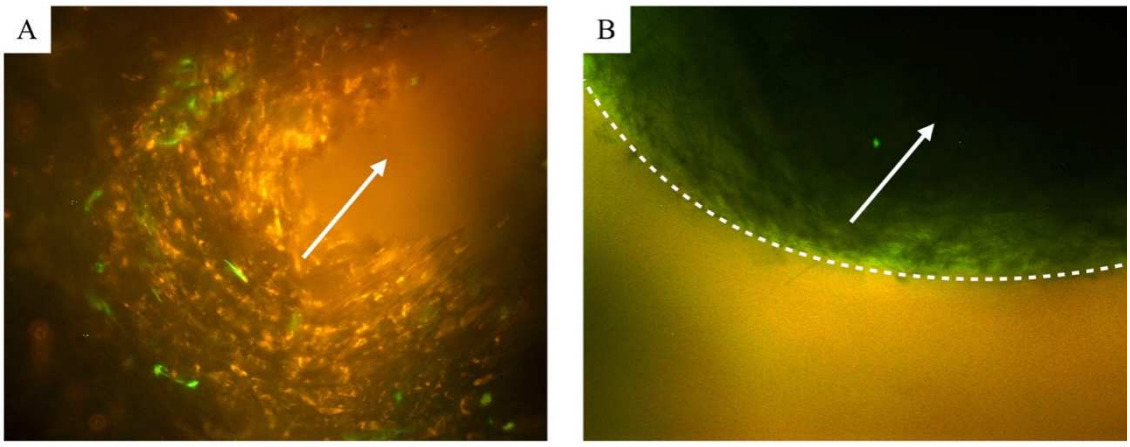


**Figure 7.** Cross sections of three-layer blood vessels. (A) 5 ml/min composite of 20 images with different focal planes from the front to the back of the freshly formed tissue. (B) 1 ml/min higher magnification image with wall exposure, white dotted line: defined separation of two layers. Both; red: RFP-SMC, green: GFP-HUVEC, white allow: flow direction.

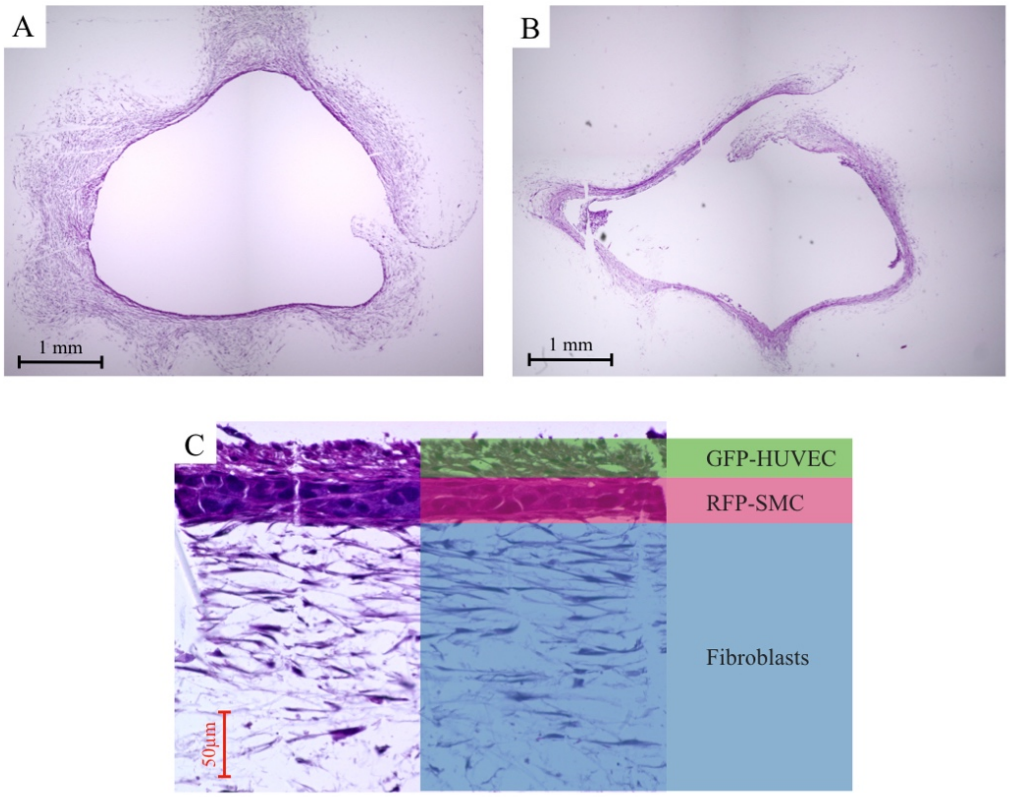


**Figure 8.** (A) Overview of a representative cross section of a 1 ml/min three-layered blood vessel stained by HE. (B) A 5 ml/min three-layered blood vessel. (C) Enlarged view of three layers. Example of thickness

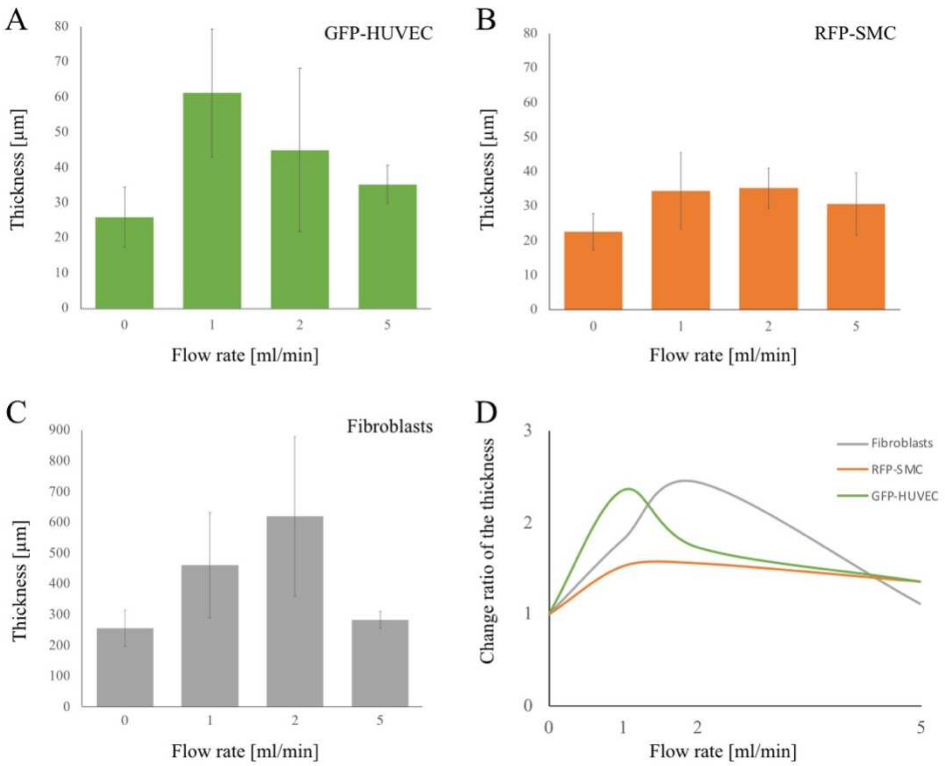


**Figure 9.** Comparison of the relative thickness for each cell layer exposed to different flow rate. (A) Endothelial cell layer. (B) Smooth muscle cell layer. (C) Fibroblast layer. (D) Change rate in layer thickness at each flow rate based on static culture of three cells types.

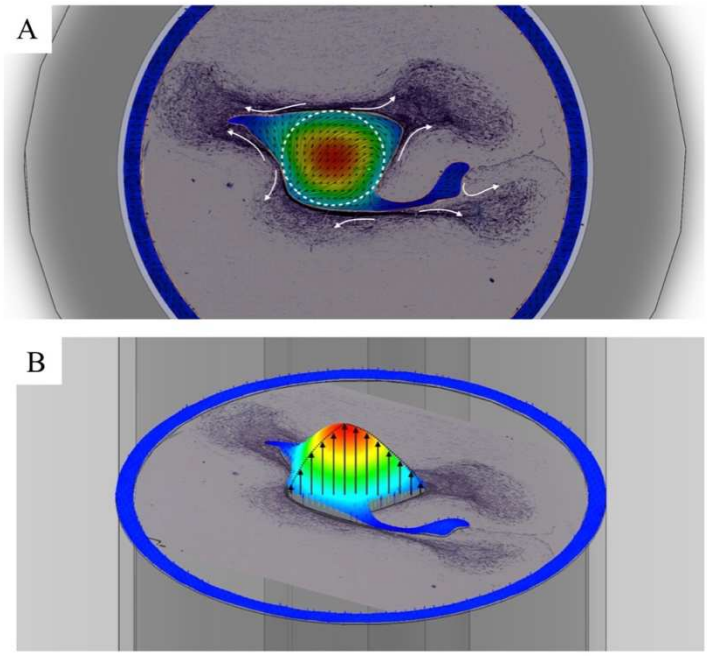


**Figure 10.** Flow Simulation of 3D Models Based on tissue cross sections by HE stained areas. (A) Cross-sectional plot of velocity gradient and streamline example. White arrows: indentation of the glass fiber scaffold and direction of cell invasion (B) Three-dimensional profile of velocity vectors.

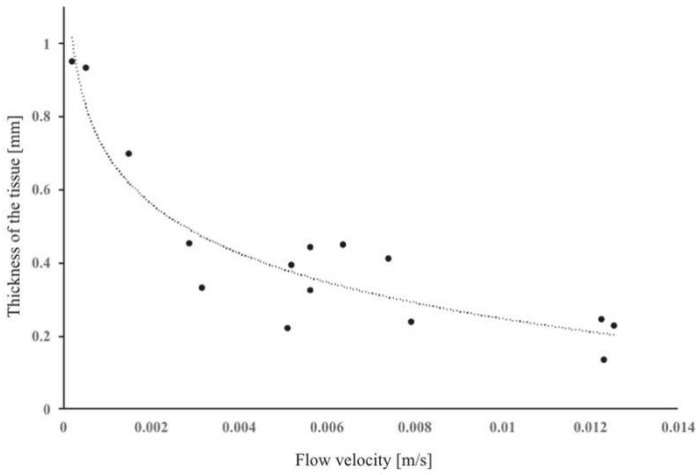


**Figure 11.** Relationship between simulated flow velocity of the media and expanded infiltration of fibroblast areas into the grass fiber.

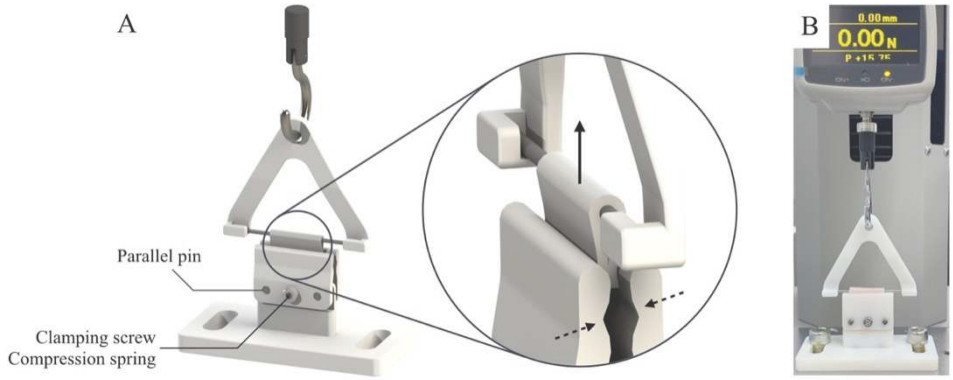


**Figure 12.** Strength measurement tester device. (A) The developed tensile holder. (B) Overall appearance of the device assembled with Load/Displacement Measurement Unit and digital force gauge.

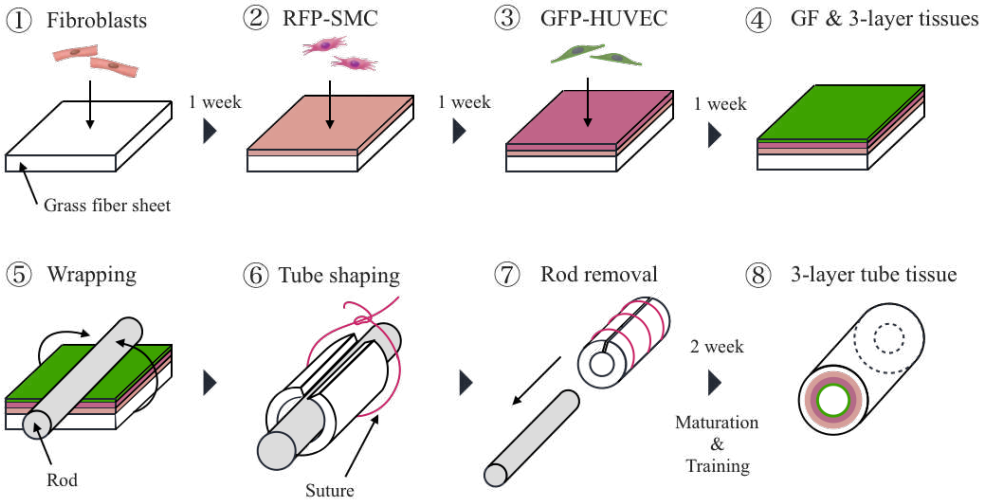


**Figure 13.** Construction method of three-layer blood vessel using glass fiber as a scaffold. 1. Fibroblast seeding. 2. Smooth muscle cell seeding on top of fibroblast layer. 3. Endothelial cells seeding onto two-layer smooth muscle cells/fibroblast structure. 4. Layer structure conditioning and tissue maturation. 5. Wrapping the flat sheet around the metal rod to form tubular shape. 6. Holding the tube shape with surgical suture. 7. Rod removal/central channel formation. 8. Formed three-layer blood vessel before tissue maturation and training.

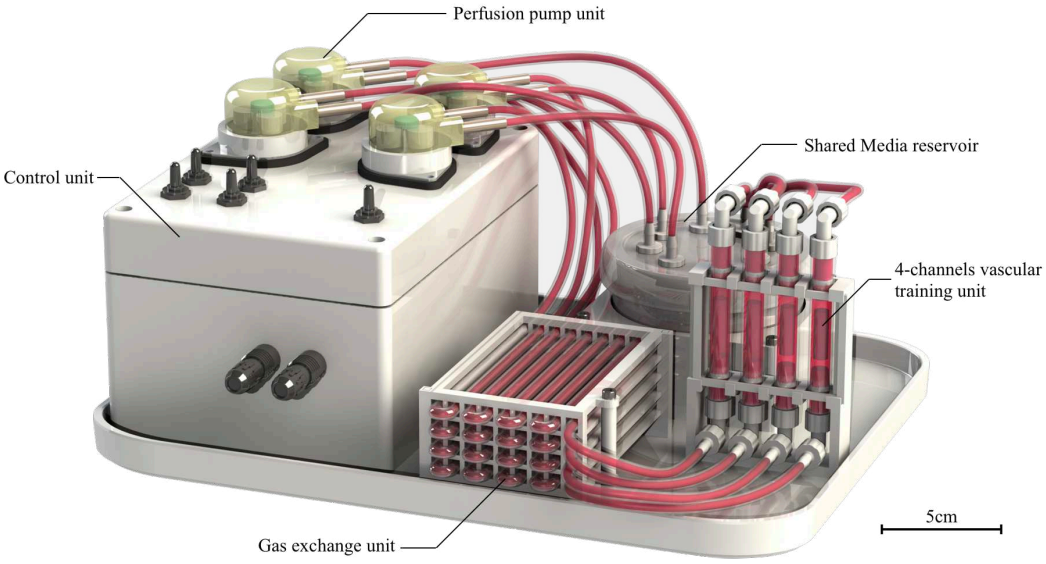


**Figure 14.** The overview of the 4-channels bioreactor for maturation of proto-tissues into the trained vascular tissue by individual training flow programs. Size bar = 5 cm.

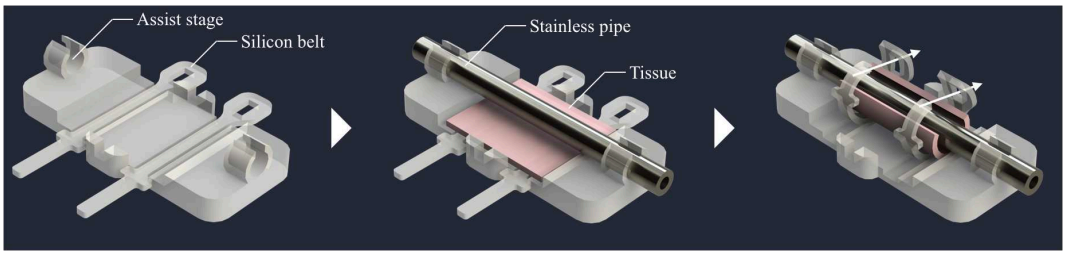


**Figure 15.** An auxiliary device for aseptic and reproducible tissue on glass fiber wrapping.

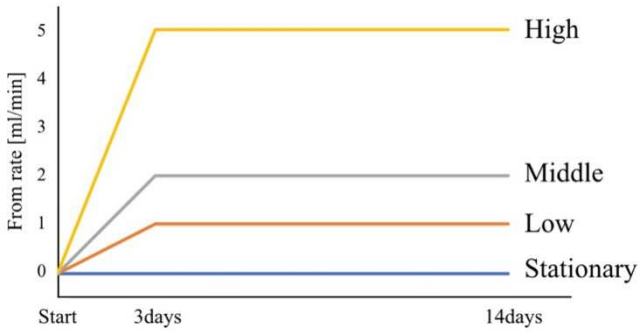


**Figure 16.** Training flow programs.

**Table 1.** Number of cells, density and survival rate

| Total Number of Cells in view field | Number of Cells / 1mm$^2$ | Survival rate [%] |
|---|---|---|
| 1226 ± 31 | 123 ± 3 | 95.8 ± 1.4 |

# Figures

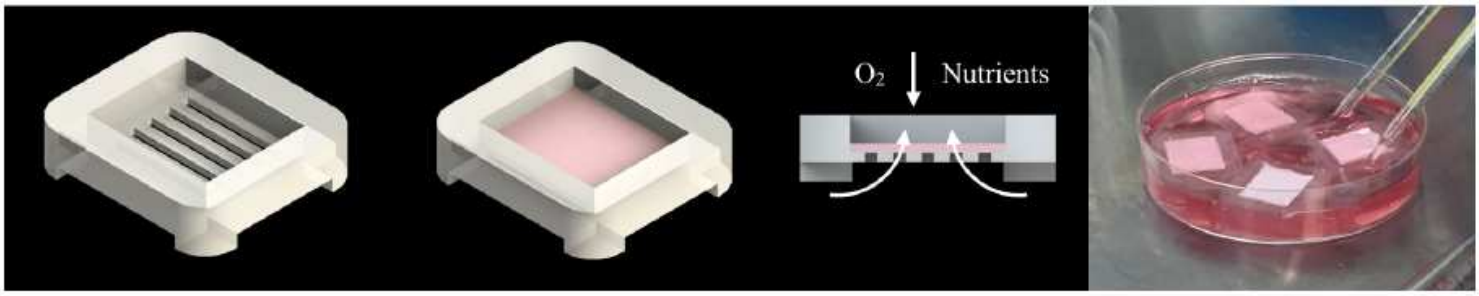


**Figure 1**

Silicone frame design for a glass fiber sheet set up and cell layer formation. Far right: Actual frames with glass fiber scaffold preconditioned in culture media.

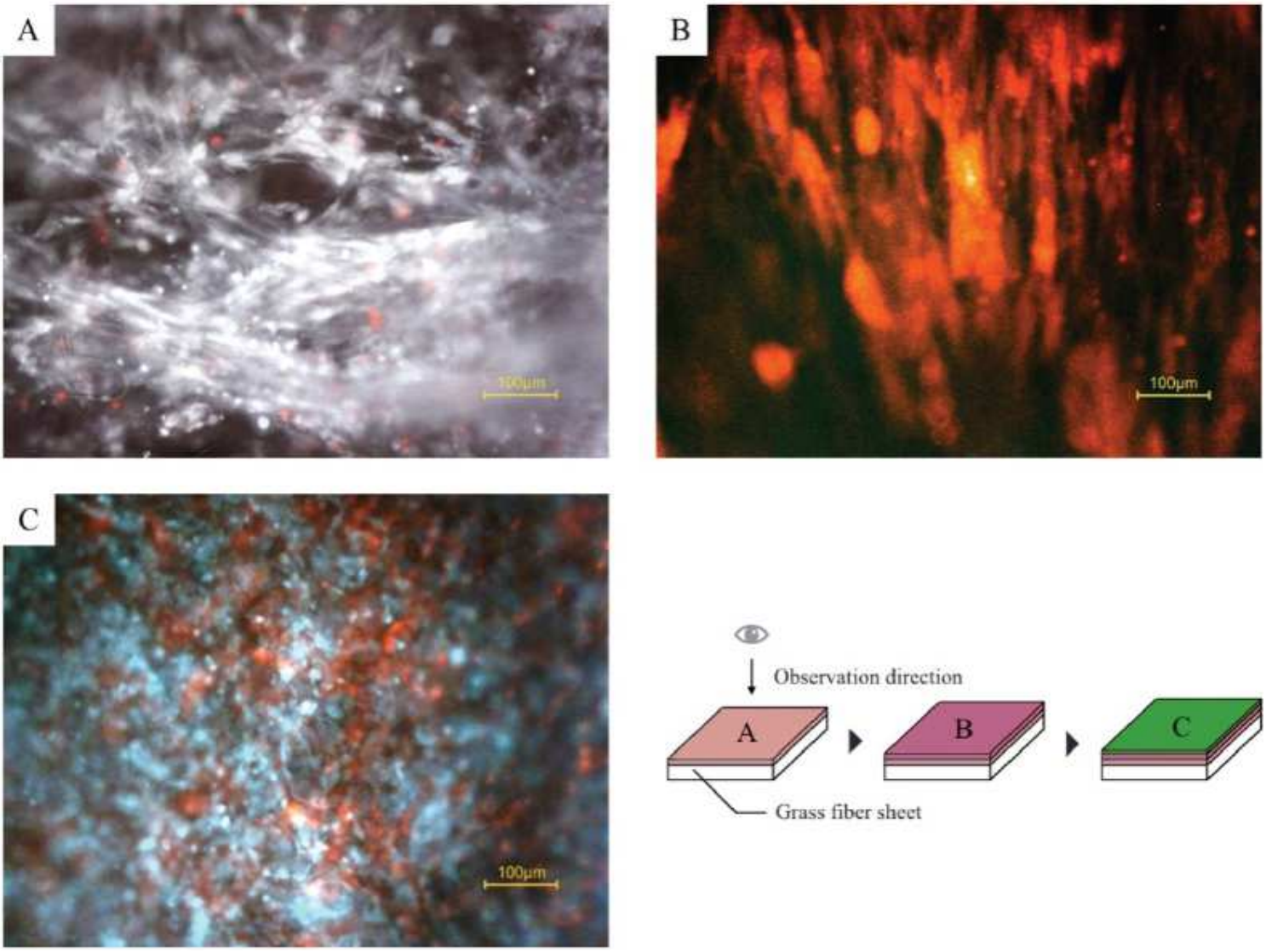


**Figure 2**

Formation of the tissue layers on a glass fiber sheet at each maturation step during sheet culture period. (A) First layer, white: fibroblasts stained by Calcein-AM, red: dead cells stained by ethidium, (B) Second layers, red fluorescent: RFP-SMCs. Fibroblasts on the background are non-fluorescent, (C) Third layers, red: RFP-SMCs, teal: GFP-HUVECs with automatic white balance. Each picture was taken under inverted fluorescent microscope after completing tissue maturation steps at weekly intervals. Fig.2C endothelial cell layer (blue) is in front of the smooth muscle cell layer (red), and the cells are close to uniformly distributed on the glass fiber.

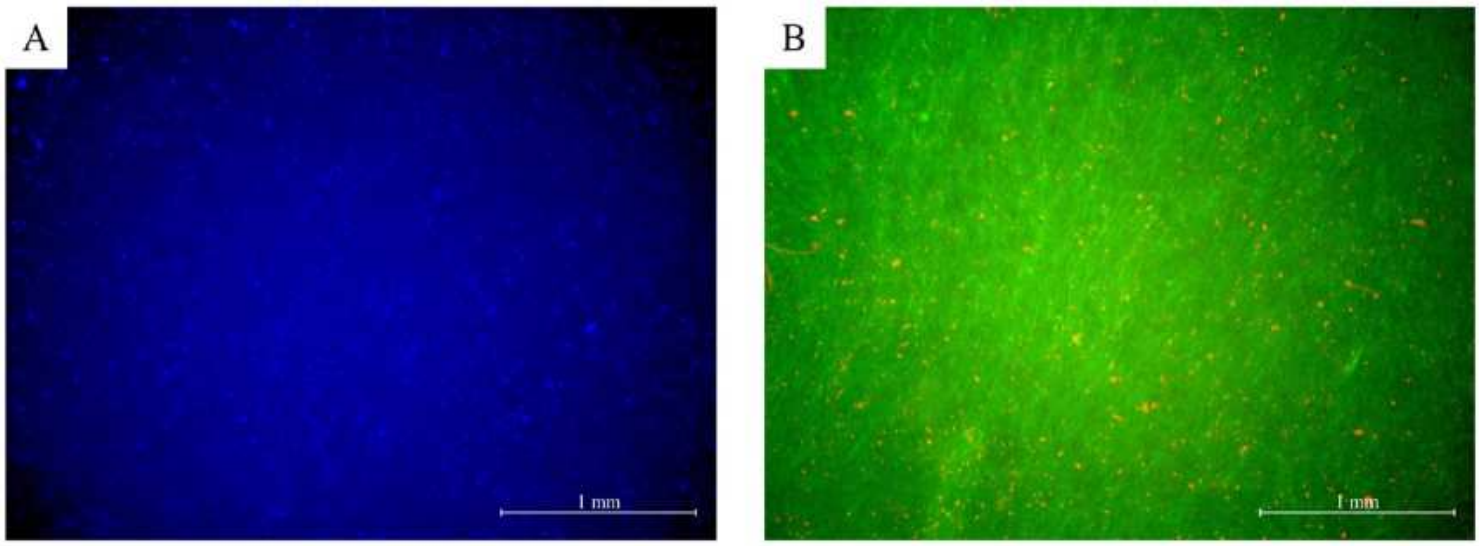


**Figure 3**

Survival of cells in the formed tissues on a GF sheet after maturation by the developed bioreactor. (A) DAPI stained nuclei, (B) Staining with Calcein-AM and Ethidium.

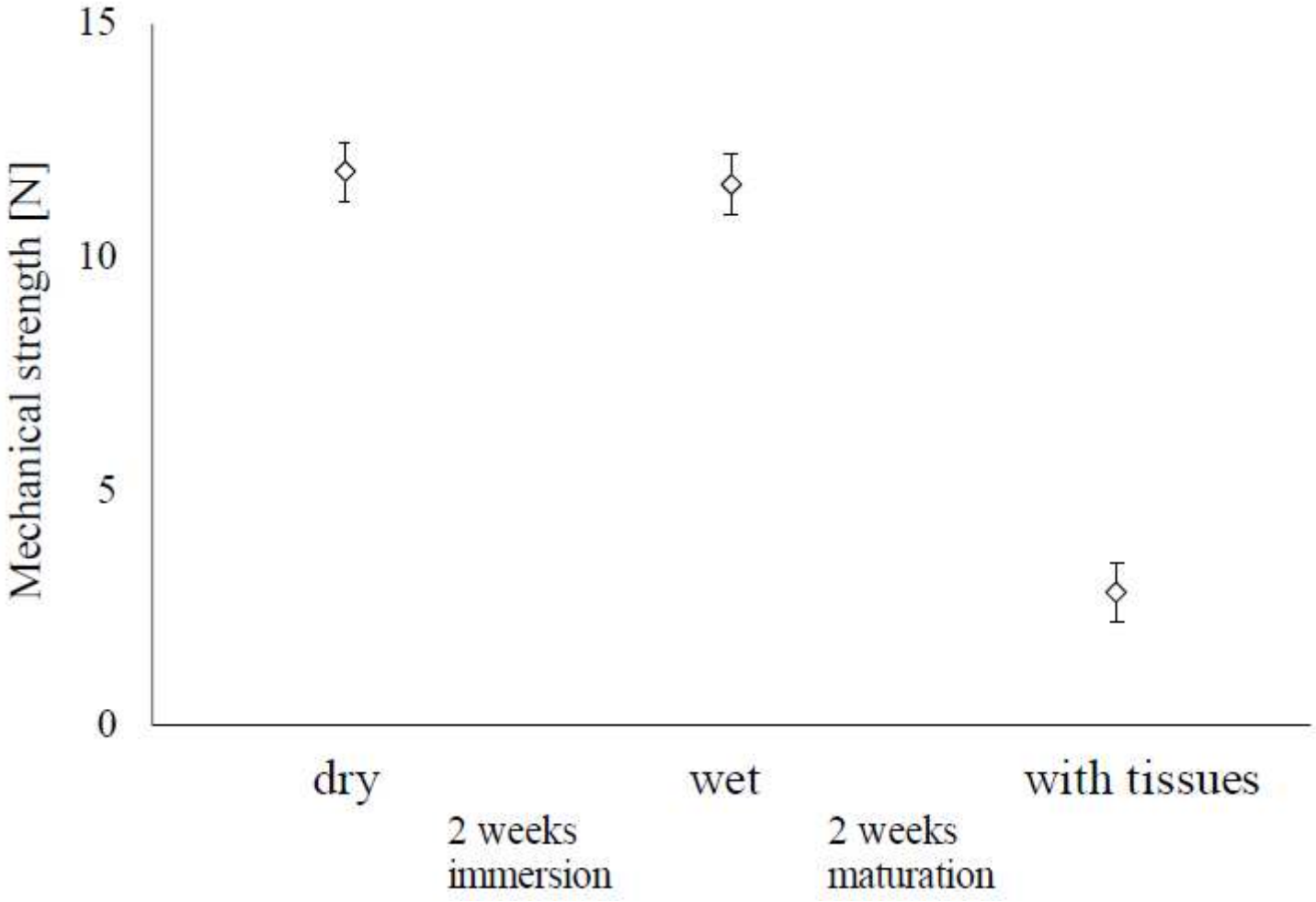


**Figure 4**

Strength measurement of the grass fiber sheet before and after tissue formation with the developed tensile tester device.

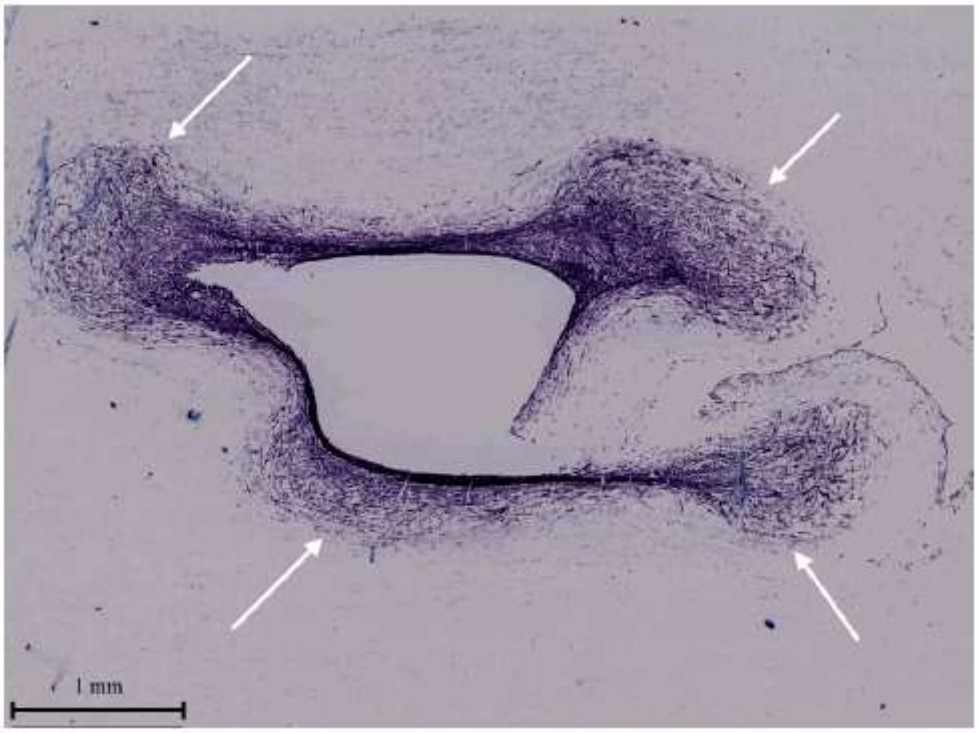


**Figure 5**

Infiltration of fibroblasts into a glass fiber. white allows: invasive growth areas.

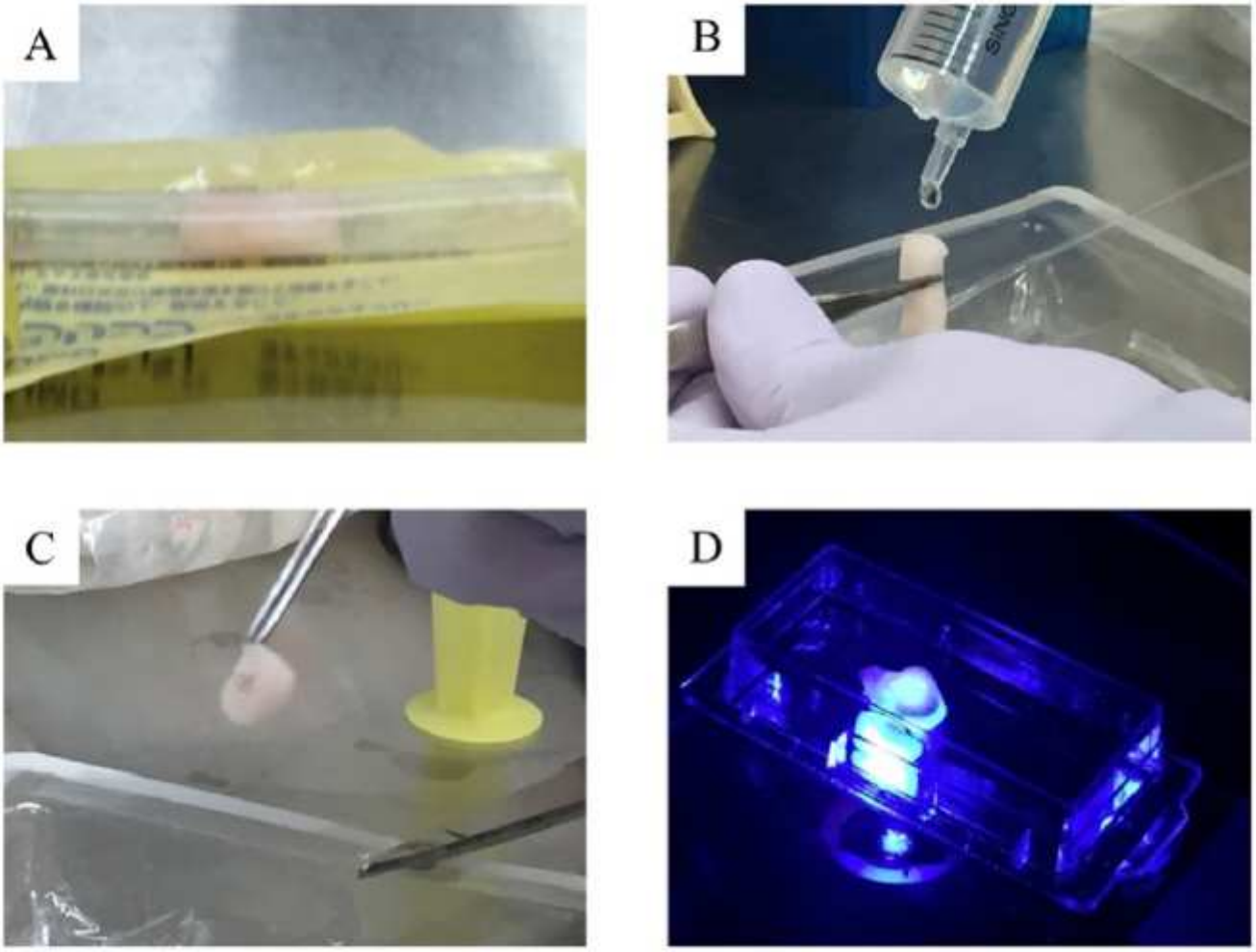

## Figure 6

Matured blood vessels after training in the bioreactor. The tubular shape could be retained without much damage by some experimental procedures. (A)Extraction (B) Washing with PBS (C) Cutting/Slicing (D) Observation

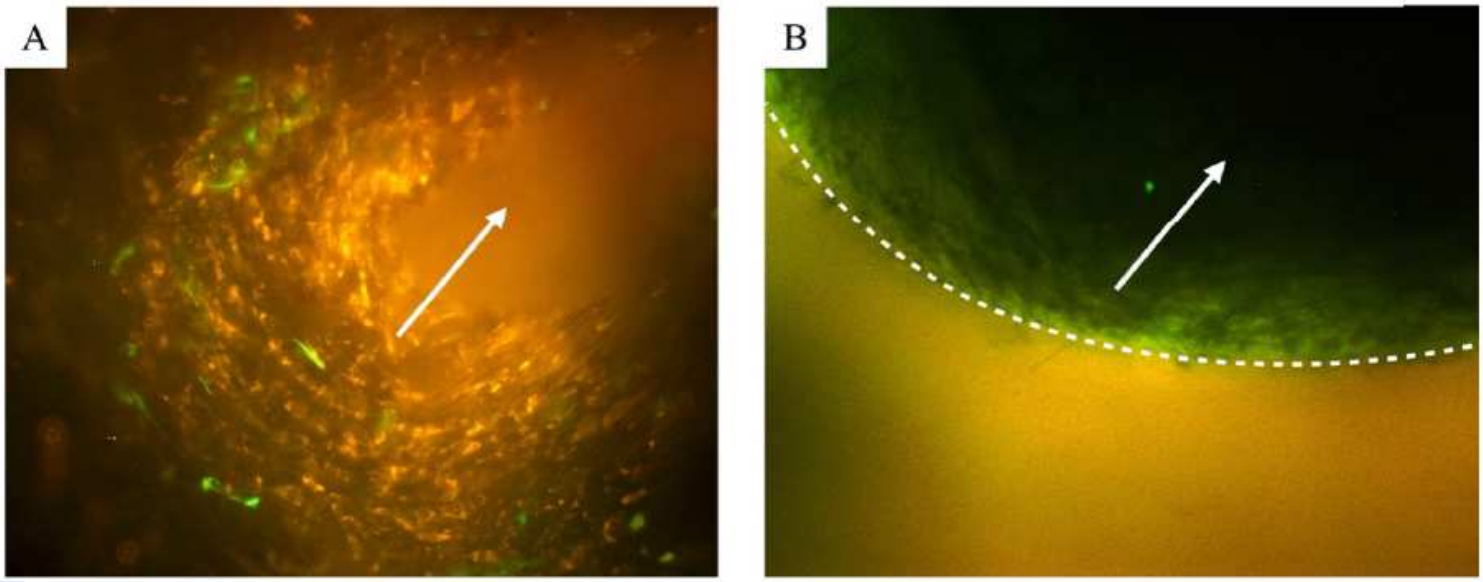


## Figure 7

Cross sections of three-layer blood vessels. (A) 5 ml/min composite of 20 images with different focal planes from the front to the back of the freshly formed tissue. (B) 1 ml/min higher magnification image with wall exposure, white dotted line: defined separation of two layers. Both; red: RFP-SMC, green: GFPHUVEC, white allow: flow direction.

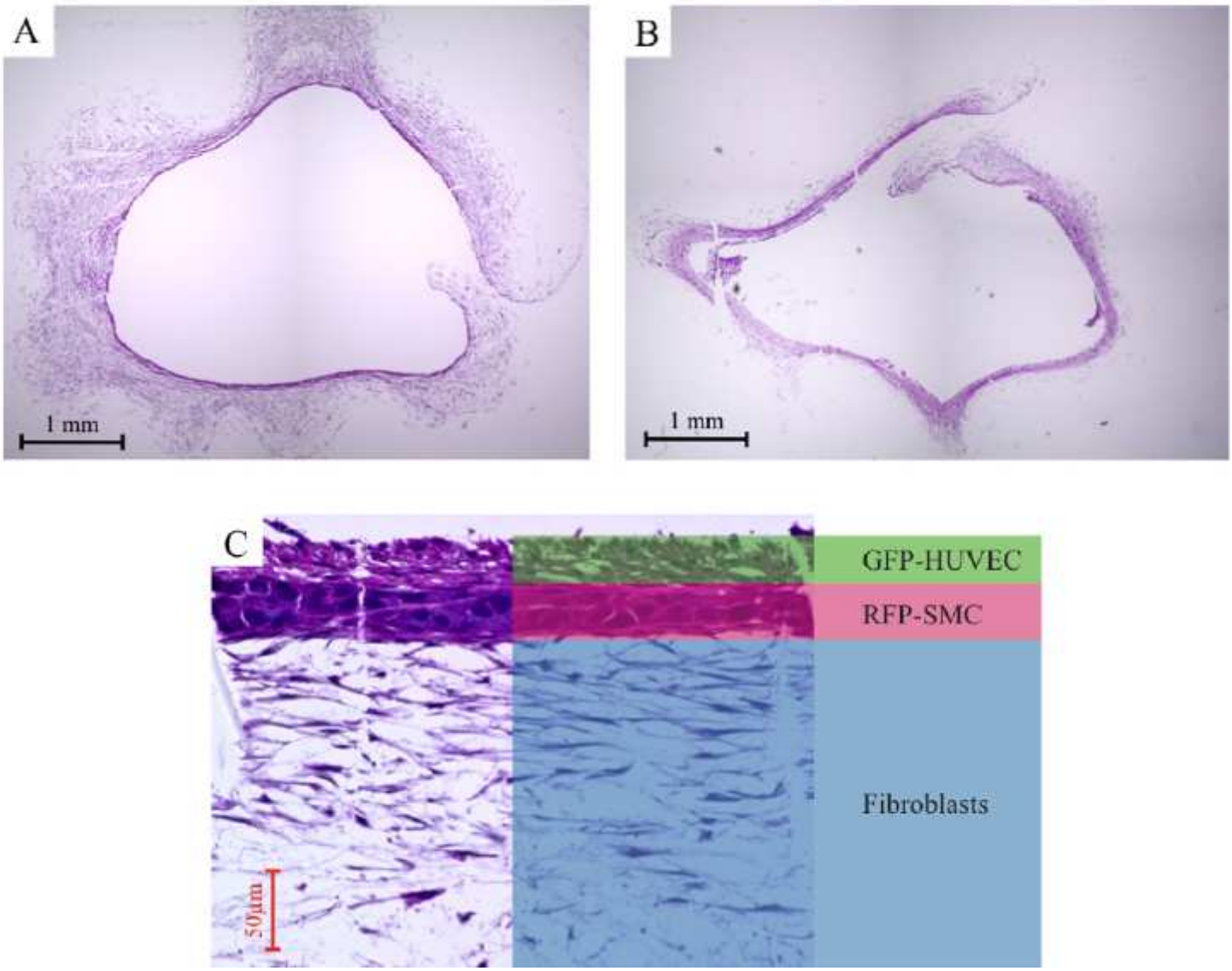


**Figure 8**

(A) Overview of a representative cross section of a 1 ml/min three-layered blood vessel stained by HE. (B) A 5 ml/min three-layered blood vessel. (C) Enlarged view of three layers. Example of thickness

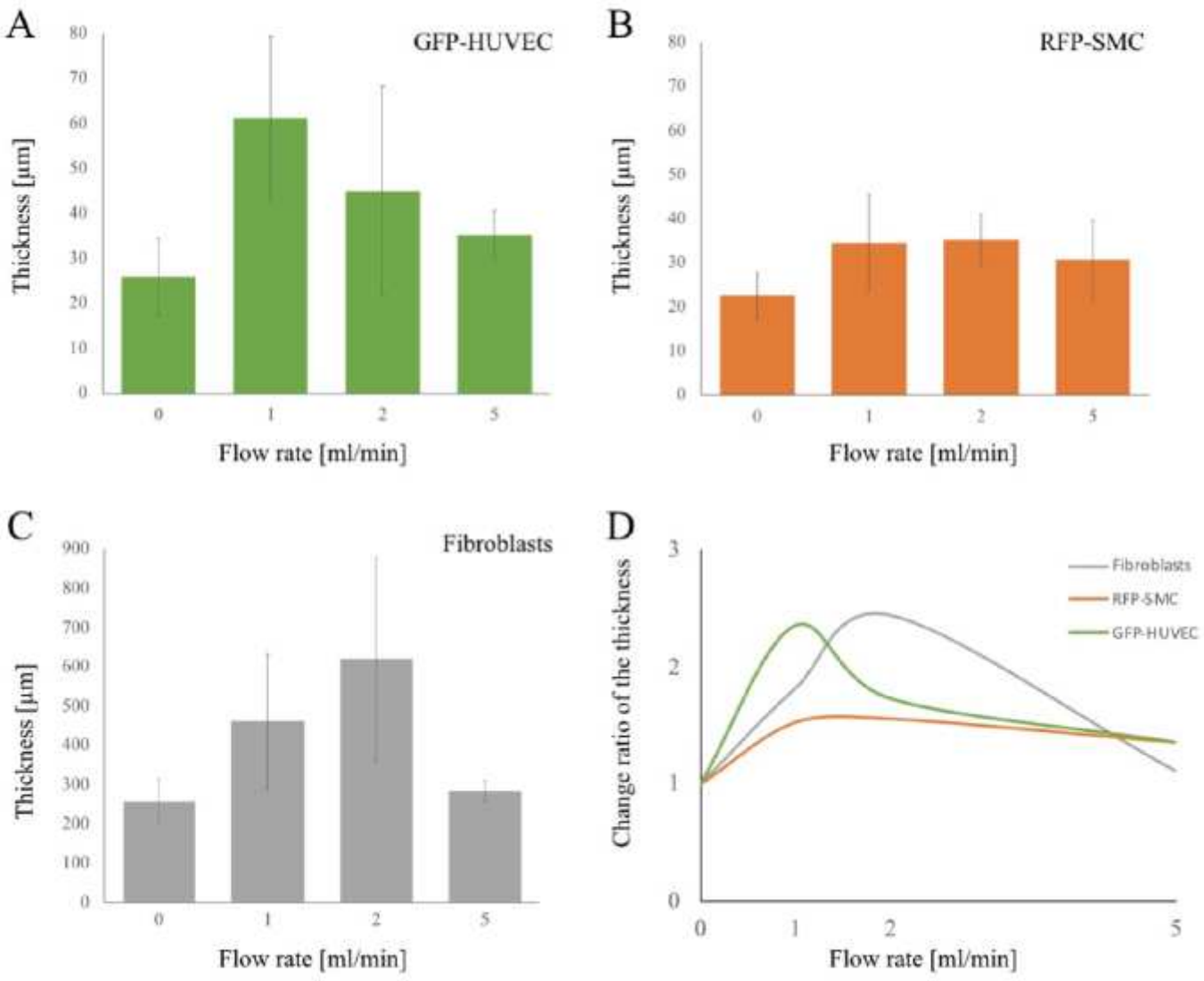


**Figure 9**

Comparison of the relative thickness for each cell layer exposed to different flow rate. (A) Endothelial cell layer. (B) Smooth muscle cell layer. (C) Fibroblast layer. (D) Change rate in layer thickness at each flow rate based on static culture of three cells types.

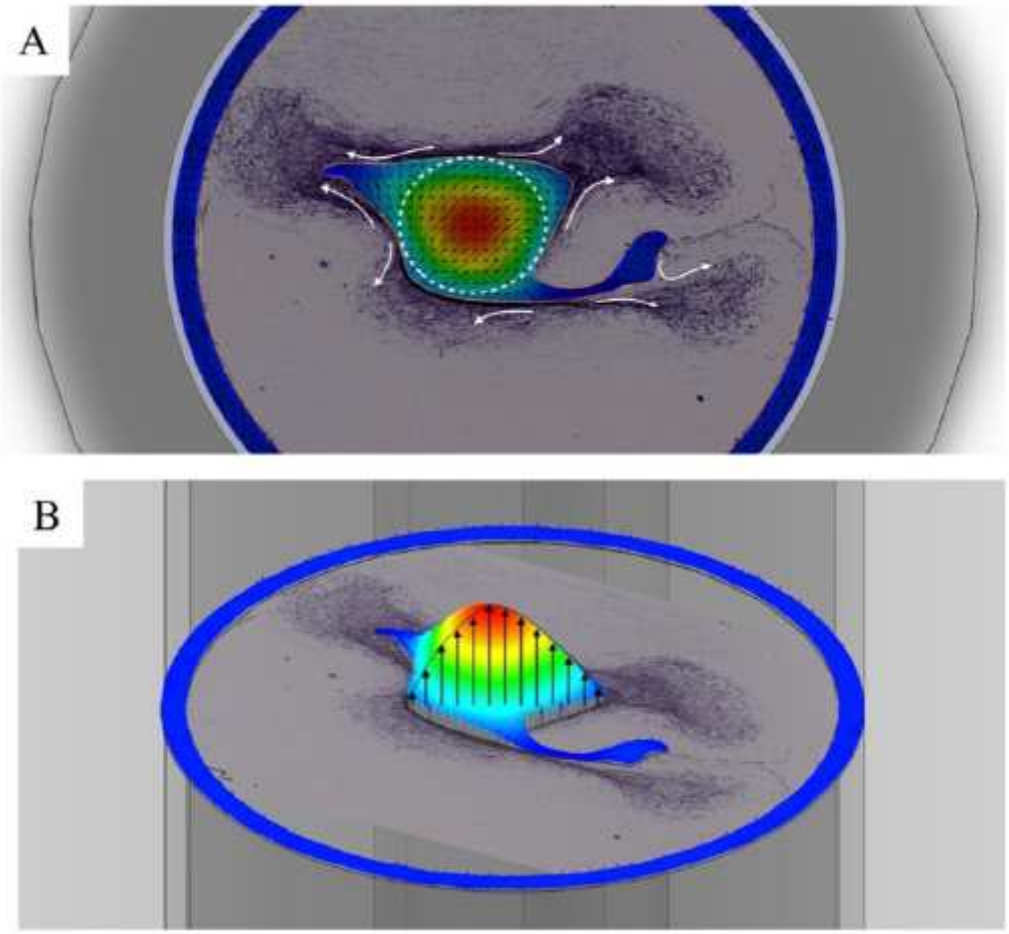


**Figure 10**

Flow Simulation of 3D Models Based on tissue cross sections by HE stained areas. (A) Crosssectional plot of velocity gradient and streamline example. White arrows: indentation of the glass fiber scaffold and direction of cell invasion (B) Three-dimensional profile of velocity vectors.

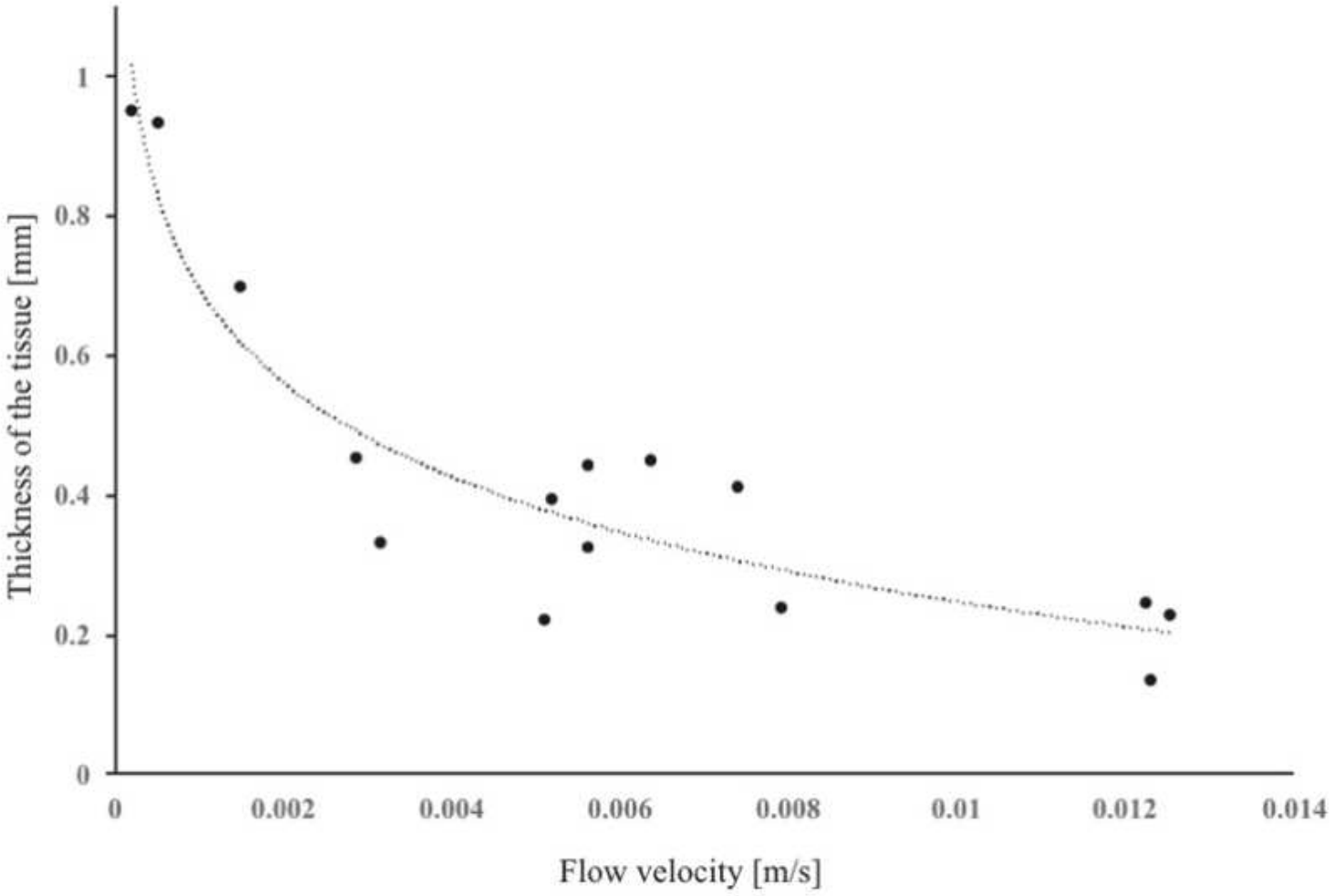


**Figure 11**

Relationship between simulated flow velocity of the media and expanded infiltration of fibroblast areas into the grass fiber.

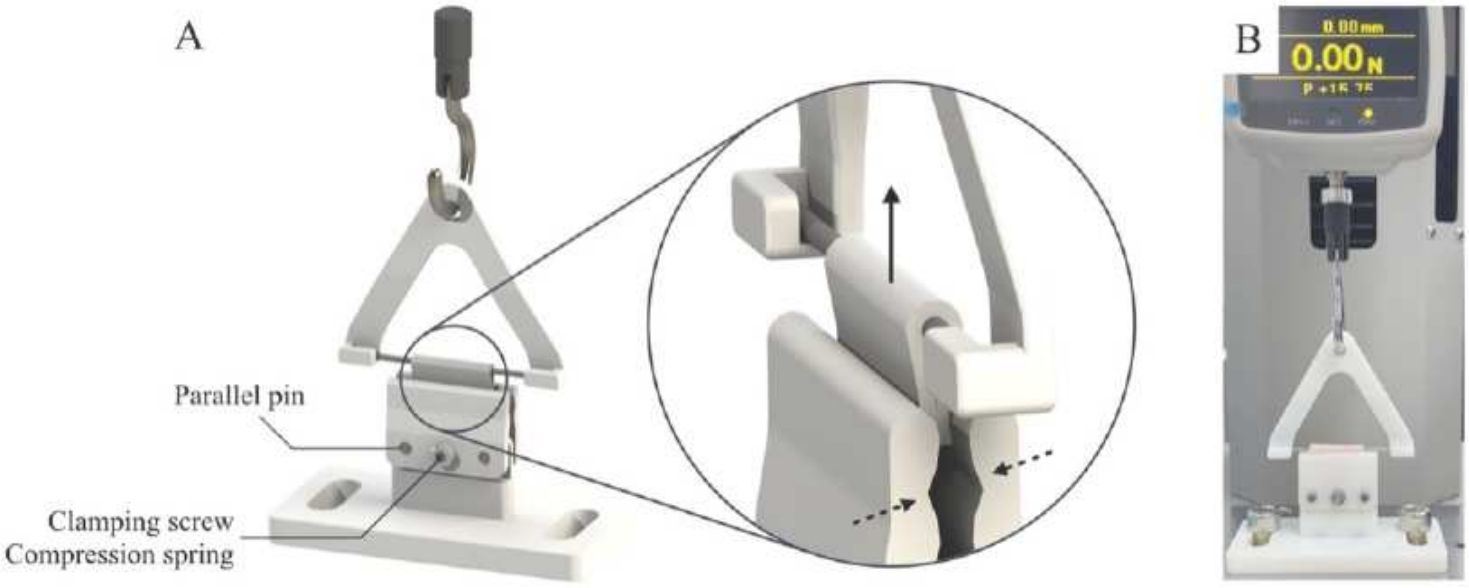


**Figure 12**

Strength measurement tester device. (A) The developed tensile holder. (B) Overall appearance of the device assembled with Load/Displacement Measurement Unit and digital force gauge.

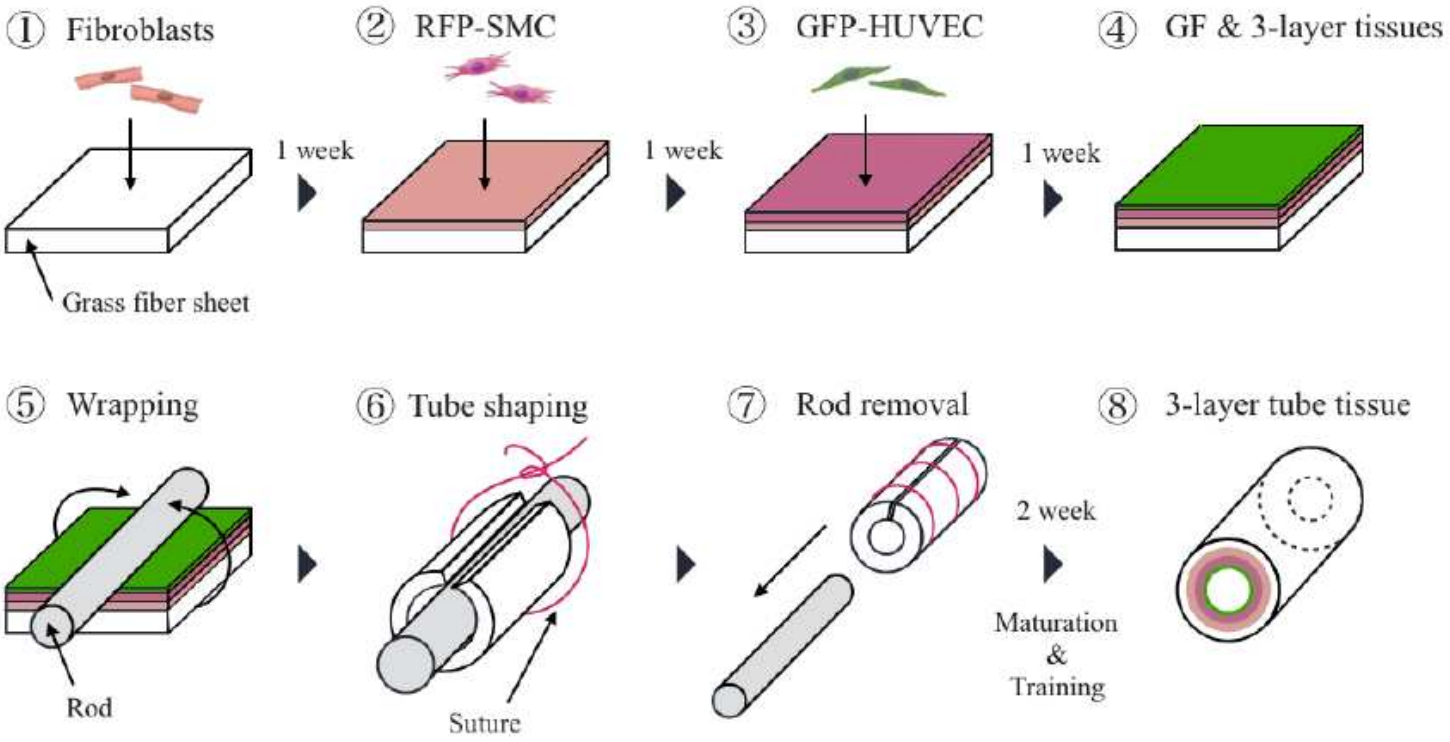


**Figure 13**

Construction method of three-layer blood vessel using glass fiber as a scaffold. 1. Fibroblast seeding. 2. Smooth muscle cell seeding on top of fibroblast layer. 3. Endothelial cells seeding onto two-layer smooth muscle cells/fibroblast structure. 4. Layer structure conditioning and tissue maturation. 5. Wrapping the flat sheet around the metal rod to form tubular shape. 6. Holding the tube shape with surgical suture. 7. Rod removal/central channel formation. 8. Formed three-layer blood vessel before tissue maturation and training.

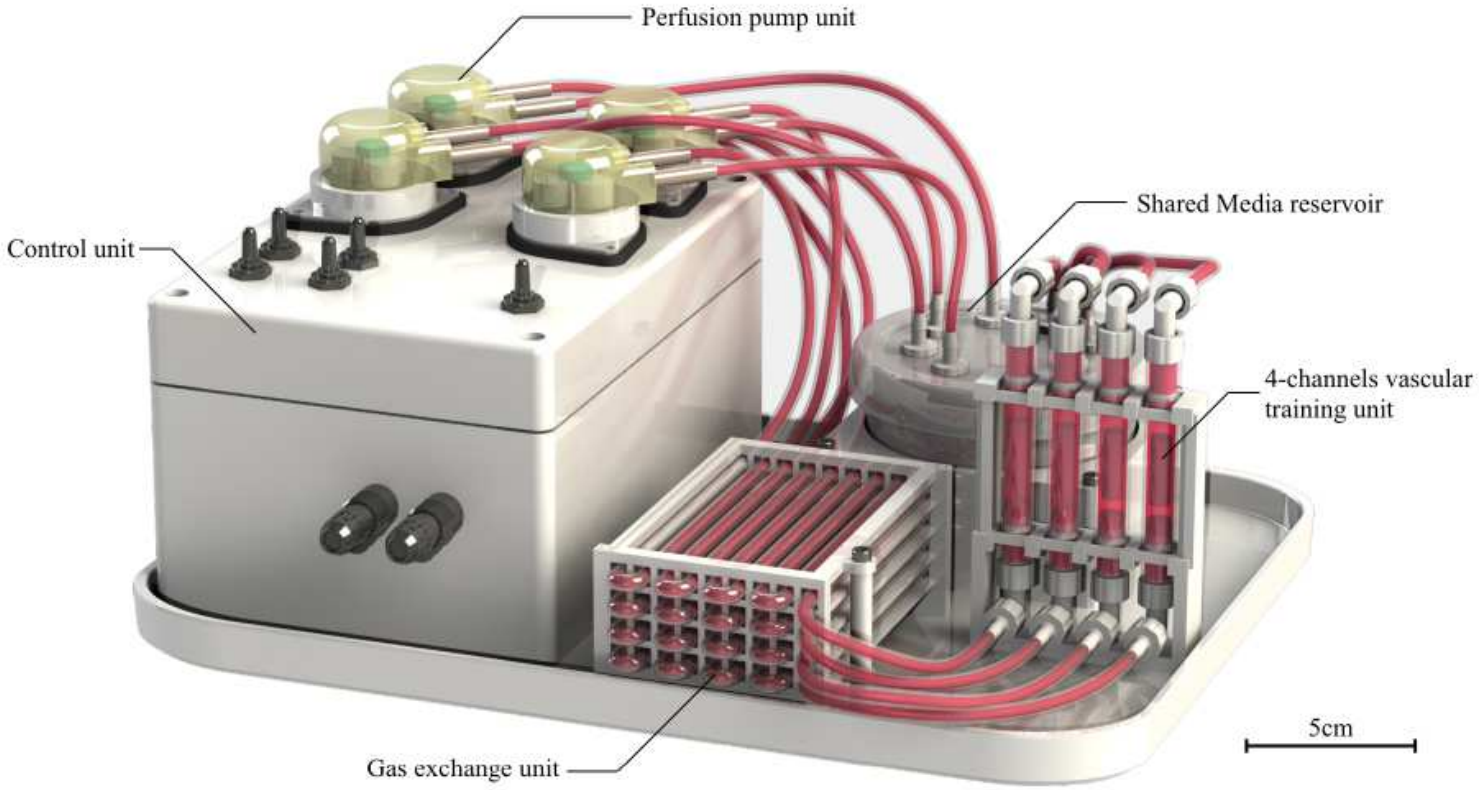


**Figure 14**

The overview of the 4-channels bioreactor for maturation of proto-tissues into the trained vascular tissue by individual training flow programs. Size bar = 5 cm.

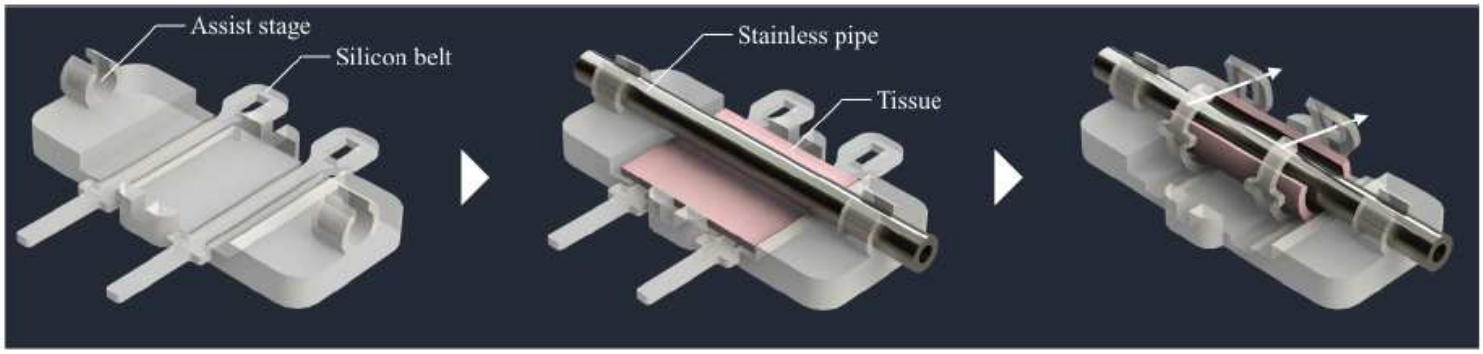


**Figure 15**

An auxiliary device for aseptic and reproducible tissue on glass fiber wrapping.


**Figure 16**

Training flow programs.